

Comprehensive genetic analysis of 57 families with clinically suspected Cornelia de Lange syndrome.

Hiromi Aoi^{1,2}, Takeshi Mizuguchi¹, Jose Ricardo Ceroni³, Veronica Eun Hue Kim³, Isabel Furquim³,
Rachel S Honjo³, Takuma Iwaki⁴, Toshifumi Suzuki², Futoshi Sekiguchi¹, Yuri Uchiyama^{1,5},
Yoshiteru Azuma¹, Kohei Hamanaka¹, Eriko Koshimizu¹, Satoko Miyatake^{1,6}, Satomi Mitsuhashi¹,
Atsushi Takata¹, Noriko Miyake¹, Satoru Takeda², Atsuo Itakura², Debora R Bertola³, Chong Ae
Kim³, Naomichi Matsumoto¹

¹Department of Human Genetics, Yokohama City University Graduate School of Medicine,
Yokohama, Japan; ²Department of Obstetrics and Gynecology, Juntendo University, Tokyo, Japan;
³Clinical Genetics Unit, Instituto da Crianca, Hospital das Clinicas HCFMUSP, Faculdade de
Medicina, Universidade de Sao Paulo, Sao Paulo, Brazil; ⁴Department of Pediatrics, University
Hospital, Faculty of Medicine, Kagawa University, Kagawa, Japan; ⁵Department of Oncology,
Yokohama City University Graduate School of Medicine, Yokohama, Japan; ⁶Clinical Genetics
Department, Yokohama City University Hospital, Yokohama, Japan.

These authors contributed equally: Chong Ae Kim, Naomichi Matsumoto

Corresponding author: Naomichi Matsumoto, Department of Human Genetics, Yokohama City

University Graduate School of Medicine, 3-9 Fukuura, Kanazawa-ku, Yokohama 236-0004, Japan.

Tel.: +81 45787 2606, Fax: +81-45 786 5219, E-mail: naomat@yokohama-cu.ac.jp

Conflict of Interest

The authors declare no conflict of interest.

1 **ABSTRACT**

2 Cornelia de Lange syndrome (CdLS) is a rare multisystem disorder with specific dysmorphic
3 features. Pathogenic genetic variants encoding cohesion complex subunits and interacting proteins
4 (e.g., *NIPBL*, *SMC1A*, *SMC3*, *HDAC8*, and *RAD21*) are the major cause of CdLS. However, there
5 are many clinically diagnosed cases of CdLS without pathogenic variants in these genes. To identify
6 further genetic causes of CdLS, we performed whole exome sequencing in 57 CdLS families,
7 systematically evaluating both single nucleotides variants (SNVs) and copy number variations
8 (CNVs). We identified pathogenic genetic changes in 36 out of 57 (63.2 %) families, including 32
9 SNVs and four CNVs. Two known CdLS genes, *NIPBL* and *SMC1A*, were mutated in 23 and two
10 cases, respectively. Among the remaining 32 individuals, four genes (*ANKRD11*, *EP300*, *KMT2A*,
11 and *SETD5*) each harbored a pathogenic variant in a single individual. These variants are known to
12 be involved in CdLS-like. Furthermore, pathogenic CNVs were detected in *NIPBL*, *MED13L*, and
13 *EHMT1*, along with pathogenic SNVs in *ZMYND11*, *MED13L*, and *PHIP*. These three latter genes
14 were involved in diseases other than CdLS and CdLS-like. Systematic clinical evaluation of all
15 patients using a recently proposed clinical scoring system showed that *ZMYND11*, *MED13L*, and
16 *PHIP* abnormality may cause CdLS or CdLS-like.

17

18

19 **INTRODUCTION**

20 Cornelia de Lange syndrome (CdLS, MIM #122470, #300590, #610759, #614701, #300882) is a rare
21 neurodevelopmental disorder characterized by dysmorphic features, prenatal onset growth restriction,
22 hirsutism, upper limb reduction defects (which range from subtle phalangeal abnormalities to
23 oligodactyly), developmental delay, and intellectual disability.¹ Prevalence of CdLS has been
24 estimated at 1/10,000 to 1/30,000 of live births.² In addition to these cardinal phenotypes, patients
25 show cardiac anomalies, gastroesophageal reflux, seizures, and behavioral problems.³ A combination
26 of signs and symptoms define the classic CdLS phenotype, which is easily recognized from birth by
27 experienced pediatricians and clinical geneticists. However, CdLS is a genetically heterogeneous
28 disorder presenting with extensive phenotypic variability from mild to severe, and with different
29 degrees of facial and limb abnormalities. In addition, CdLS clinically overlaps with several other
30 diseases including Bohring-Optiz syndrome, CHOPS syndrome, and Fryns syndrome.^{4, 5} Such
31 heterogeneity makes it difficult to clearly distinguish CdLS from other clinically overlapping diseases.
32 Recently, an international consensus group provided clinical criteria for CdLS.⁶ This criteria uses a
33 scoring system comprised of cardinal and suggestive features.

34 To date, pathogenic variants in at least 15 genes are known to cause CdLS.⁷⁻¹⁰ In this regard, cohesin
35 complex or its functionally related genes (e.g., nipped B-like protein [*NIPBL*], structural
36 maintenance of chromosome 1A [*SMC1A*], *SMC3*, histone deacetylase 8 [*HDAC8*], and RAD21

37 cohesin complex component [*RAD21*]) have been implicated. Approximately 60% of CdLS patients
38 harbor various *NIPBL* variants.¹ Cohesin is a multisubunit protein complex consisting of four core
39 proteins: SMC1, SMC3, RAD21, and stromal antigen (STAG).⁶ Chromatin loading of cohesion is
40 regulated by NIPBL.¹¹ The cohesin complex plays a significant role in mediating sister chromatid
41 cohesion, DNA double-strand break repair, transcriptional regulation, and chromatin organization.
42 Abnormalities of cohesion complex and its related genes in humans are known as cohesinopathy.¹²
43 In addition, variants in *AFF4*, *ANKRD11*, *ARID1B*, *BRD4*, *EP300*, *ESPL1*, *KMT2A*, *PDGFRB*,
44 *SETD5*, and *TAF6* also cause a CdLS-like phenotype.^{7-9, 13-15}
45 In this study, we investigated 57 clinically suspected CdLS individuals by whole exome sequencing
46 (WES). Genetic findings, including single nucleotide variants (SNVs) and copy number variations
47 (CNVs), together with clinical features obtained using recent clinical criteria are presented and
48 discussed.

49

50 **METHODS**

51 **Subjects**

52 In this study, 57 patients were recruited from 57 families, consisting of 56 Brazilian and one
53 Japanese patients. Most of the Brazilian patients were referred by the Brazilian Association of
54 Cornelia de Lange Syndrome (CdLS Brazil) and had the clinical diagnosis suspected by

55 pediatricians and/or geneticists from all over the country based on distinctive features such as
56 synophrys, arched eyebrows, long philtrum, upper limb abnormalities, and hirsutism. For
57 comparison of clinical manifestations within our cohort and genotype–phenotype correlations,
58 clinical details (including atypical symptoms) were retrospectively reviewed based on recent clinical
59 criteria reported by Kline *et al.*⁶ Clinical information was obtained from all 57 patients (Table S1).
60 Peripheral blood leukocytes were collected from patients and their parents after obtaining informed
61 consent. Parental samples were available except for five families (Families 6, 7, 10, 22, and 30). This
62 study was approved by the Institutional Review Boards of Yokohama City University, Faculty of
63 Medicine, and University of Sao Paulo, Faculty of Medicine.

64

65 **Whole exome sequencing**

66 Genomic DNA was extracted from whole blood sample using QuickGene-610L (Fujifilm, Tokyo,
67 Japan) according to the manufacturer’s protocol. Genomic DNA was sheared using a S220 Focused-
68 ultrasonicator (Covaris, Woburn, MA, USA) and captured using the SureSelect Human All Exon V6
69 Kit (Agilent Technologies, Santa Clara, CA, USA). Paired-end libraries were sequenced on an
70 Illumina HiSeq 2500 platform (Illumina, San Diego, CA, USA) with 101-bp paired-end reads.
71 Quality-controlled reads were aligned to the human reference genome (UCSC hg19, NCBI build
72 37.1) using NOVOALIGN (<http://www.novocraft.com/products/novoalign/>). After removal of

73 polymerase chain reaction (PCR) duplications using Picard (<http://broadinstitute.github.io/picard/>),
74 variants were called using Genome Analysis Tool Kit (GATK)
75 (<https://software.broadinstitute.org/gatk/index.php>). Called variants were annotated using
76 ANNOVAR (<http://annovar.openbioinformatics.org/en/latest/>). Exonic and intronic variants within
77 30 bp from exon–intron boundaries were examined. Synonymous variants and variants with minor
78 allele frequencies ≥ 0.01 in our in-house exome database of 575 Japanese individuals or control
79 population databases (including the Exome Aggregation Consortium Browser population (ExAC)
80 [<http://exac.broadinstitute.org/>] and National Heart, Lung, and Blood Institute (NHLBI) exome
81 variant server [<http://evs.gs.washington.edu/EVS/>]) were removed. Missense variants were evaluated
82 using Sorting Intolerant From Tolerant (SIFT) (<http://sift.jcvi.org/>), Polymorphism Phenotyping v2
83 (Polyphen-2) (<http://genetics.bwh.harvard.edu/pph2/>), and MutationTaster
84 (<http://MutationTaster.org/>).

85 In particular, the focus was on five CdLS genes (*NIPBL*, *SMC1A*, *SMC3*, *HDAC8*, and *RAD21*) and
86 10 CdLS-like genes (*AFF4*, *ANKRD11*, *ARID1B*, *BRD4*, *EP300*, *ESPL1*, *KMT2A*, *PDGFRB*,
87 *SETD5*, and *TAF6*). Candidate variants were validated by Sanger sequencing. Additionally, *de novo*
88 occurrences were validated when parental samples were available. Parentage was confirmed by
89 analyzing 12 microsatellite markers with Gene Mapper software v4.1.1 (Life Technologies Inc.,
90 Carlsbad, CA, USA). The WES performance is summarized in Supplementary Information (Table

91 S2).

92

93 **Real-time reverse transcription PCR**

94 To detect aberrant transcripts caused by splice site mutations, reverse transcription PCR (RT-PCR)

95 was performed using total RNA extracted from patient derived lymphoblastoid cell lines. Total RNA

96 was extracted using the RNeasy Plus Mini Kit (Qiagen, Hilden, Germany) and reverse-transcribed

97 into cDNA using the Super Script First Strand Synthesis System (Takara, Kyoto, Japan). Resultant

98 cDNA was used as a template for PCR. PCR amplicons were subjected to Sanger sequencing and

99 aberrant transcripts were characterized. For RT-PCR analysis of *NIPBL*, the forward and reverse

100 primers were: 5'-GAACACTTCAGTTGCTGCAAA-3' and

101 5'-CGTTTCCTAGAGGATTCAAAAGC-3' in Patient 15 with c.3121+1G>A, and

102 5'-TCATCCAGTTCAGTGTGTGC-3' and 5'-TCTCAATGACCCTGAAGTGC-3' in Patient 28 with

103 c.7410+4A>G.

104

105 **WES-based CNV analysis**

106 Using WES data, CNVs were analyzed by two algorithms: the eXome Hidden Markov Model

107 (XHMM), and a program based on relative depth of coverage ratio, developed by Nord *et al.* (Nord

108 program).^{16,17} For genome-wide screening, XHMM data were first examined in each patient. If

109 causative CNVs were detected using XHMM, altered copy numbers of such regions were further
110 verified using the Nord program. In addition, CNVs at five CdLS genes and 10 CdLS-like genes (see
111 WES section above) were tested by the Nord program.

112

113 **Quantitative polymerase chain reaction**

114 Candidate CNVs were validated by quantitative polymerase chain reaction (qPCR). Real-time qPCR
115 was performed to examine genomic DNA copy number at *NIPBL*, *C5orf42*, *MED13L*, *SMARCA2*,
116 *FREMI*, and *EHMT1* target loci. QuantiFast SYBER Green PCR kit (Qiagen) was used for real-time
117 quantification with amplification monitored on a Rotor-Gene Q real-time PCR cyclers (Qiagen).
118 Relative ratios of genomic DNA copy number were calculated using the standard curve method with
119 Rotor-Gene 6000 Series Software 1.7 (Qiagen) by normalizing with autosomal internal control loci
120 (*STXBPI* and/or *FBNI*) and also compared to an unrelated control individual. Information of all
121 primers is available on request.

122

123 **RESULTS**

124 **Flowchart of this study**

125 A flowchart of this study is shown in Figure 1. Because of the genetic and clinical heterogeneity of
126 CdLS, we directly employed WES to effectively screen pathogenic variants in patients with

127 clinically suspected CdLS. To detect variants in CdLS, CdLS-like, or other possible genes, all 57
128 patients were analyzed based on autosomal dominant (*de novo*), autosomal recessive, and X-linked
129 modes of inheritance. Based on American College of Medical Genetics and Genomics (ACMG)
130 guidelines¹⁸, we identified 29 pathogenic or likely pathogenic SNVs in two CdLS genes (*NIPBL* and
131 *SMCIA*) and four CdLS-like genes (*ANKRD11*, *EP300*, *KMT2A*, and *SETD5*) (Figure 1). WES-
132 based CNV analysis in 28 SNV-negative patients detected pathogenic CNVs in four patients (4/57
133 [7.0%]), involving *NIPBL*, *MED13L*, *EHMT1*, and 9q deletion (Figure 1). The remaining 24 cases
134 had neither pathogenic SNVs nor CNVs. Consequently, these cases were subjected to trio-based
135 analysis, except for two cases whose parental samples were unavailable. We detected three
136 pathogenic variants in genes associated with diseases other than CdLS and CdLS-like: *ZMYND11*,
137 *MED13L*, and *PHIP*. Altogether, if all abnormalities were included, we identified pathogenic or
138 likely pathogenic variants in 36 out of 57 cases (63.2%) (Figure 1). Thirty-one of 36 variants
139 occurred *de novo*, unless biological parental samples were unavailable. One variant was inherited
140 from a mosaic mother (Patient 53). Twenty-three of 32 pathogenic SNVs were novel (Table 1).

141

142 **Pathogenic SNVs in CdLS genes**

143 We detected 22 pathogenic SNVs in *NIPBL* (22/57 [38.6%]) and two in *SMCIA* (2/57 [3.5%]) (Table
144 1 and Figure 1). Among 22 *NIPBL* SNVs, 14 were novel. Meanwhile, NM_0133433.3:c.6893G>A,

145 p.Arg2298His was repeatedly detected (Patients 2 and 50). Three splice site variants in *NIPBL*
146 (NM_0133433.3:c.3121+1G>A, c.7410+4A>G, and c.5329-15A>G) were detected in Patients 15,
147 28, and 54, respectively. These variants were previously described, and only c.5329-15A>G was
148 shown to result in abnormal splicing.¹⁹⁻²¹ The other c.3121+1G>A and c.7410+4A>G mutations
149 were never examined at cDNA level.¹⁹⁻²¹ Therefore, by RT-PCR using cDNA derived from
150 lymphoblastoid cells, we confirmed aberrant splicing in both Patient 15, with c.3121+1G>A, and
151 Patient 28, with c.7410+4A>G (Figure S1). Regarding the two missense variants in *SMCIA*,
152 NM_006306.3:c.1152C>G, p.Lys362Asn was novel.

153

154 **Pathogenic SNVs in CdLS-like genes**

155 We also detected pathogenic variants in four CdLS-like genes: *ANKRD11* (2/57 [3.5%]), *EP300*
156 (1/57 [1.8%]), *KMT2A* (1/57 [1.8%]), and *SETD5* (1/57 [1.8%]) (Table 1 and Figure 1), whose
157 pathogenic variants are known to cause KBG syndrome (MIM #148050), Rubinstein–Taybi
158 syndrome 2 (MIM #613684), Wiedemann–Steiner syndrome (MIM #605130), and mental
159 retardation autosomal dominant 23 (MIM #615761), respectively. These disorders all share
160 overlapping clinical features with CdLS. All five variants were novel, occurring *de novo* except for
161 an *EP300* variant, which was due to unavailable parental samples. According to the ACMG
162 guideline, the *EP300* variant can be classified as likely pathogenic since it is protein length changing

163 mutation due to in-frame deletion (PM4), it is absent from control (including the ExAC, NHLBI, and
164 gnomAD [<https://gnomad.broadinstitute.org/>]) (PM2), it is predicted to be deleterious by PROVEAN
165 [http://provean.jcvi.org/seq_submit.php] and CADD [<https://cadd.gs.washington.edu/>] with a score
166 of 23.6 and 21.1, respectively (PP3), and the phenotype of patient is considered reasonable as
167 Cornelia de Lange syndrome-like (PP4).

168

169 **Pathogenic CNVs**

170 Using the XHMM and Nord program, we detected four pathogenic CNVs in four patients (Table 1
171 and Figure 1). These were confirmed by qPCR. Patient 9 has a 94-kb deletion at 5p13.2,
172 encompassing exons 22 to 47 of *NIPBL* and the last exon of *C5orf42* (Figure S2a). Partial deletions
173 of *NIPBL* have been reported in patients with CdLS, and *NIPBL* haploinsufficiency is apparently
174 deleterious.²² Patient 34 has a 4.2-Mb deletion at 12q24.1-q24.23, which contains 40 genes including
175 the entire *MED13L* gene (Figure S2b). Patient 51 has a 14.1-Mb deletion at 9p24.3-p22.3, involving
176 44 genes and an adjacent 571-kb duplication at 9p22.3, altogether encompassing four genes (Figure
177 S2c). Patient 52 has a 774-kb deletion at 9q34.3, containing 14 genes including the entire *EHMT1*
178 gene (Figure S2d).

179

180 **Variants in genes associated with diseases other than CdLS and CdLS-like**

181 By trio-based analysis, we identified pathogenic or likely pathogenic variants in *ZMYND11*, *MED13L*,
182 and *PHIP*. These variants are involved in other diseases, but never CdLS or CdLS-like.

183 A novel *ZMYND 11* frameshift variant (NM_006624.5:c.1438delG, p.Asp480Thrfs*3) was detected
184 in Patient 53, who had typical CdLS features including left hand oligodactyly (Tables 1 and S1, and
185 Figure 2a–e). Based on apparent double sequences implying low mutant allele peaks in the
186 electropherogram of the mother, maternal mosaicism of this variant was examined (Figure S3). Deep
187 sequencing of PCR products encompassing the maternal variant confirmed mosaicism
188 (mutant/mutant+wild-type reads = 2835/27596 [10.3%]), while Patient 53 showed heterozygosity
189 (mutant/mutant+wild-type reads = 12514/27211 [46.0%]) (Table S3). By TA cloning of PCR products
190 spanning the maternal variant, wild-type and mutant alleles were clearly recognized by Sanger
191 sequencing (Figure S3), yet the mother had no CdLS-like features. *ZMYND11* has been reported as a
192 critical gene for 10p15.3 microdeletion syndrome, including neurodevelopmental disorder,
193 characteristic dysmorphic features, and other more frequent symptoms, such as behavioral
194 disturbances, hypotonia, seizures, low birth weight, short stature, genitourinary malformations, and
195 recurrent infections.²³

196 A novel *MED13L* missense mutation, NM_015335.4:c.6485C>A, p.Thr2162Lys was detected in
197 Patient 5 (Table S4). *MED13L* variants cause distinctive dysmorphic features and mental retardation
198 with or without cardiac defects (MIM #608771), known as *MED13L* haploinsufficiency syndrome.²⁴

199 The missense variant identified here is novel, but another variant at the same nucleotide position was
200 previously identified, which leads to a different amino acid substitution (NM_015335.4:c.6485C>T,
201 p.Thr2162Met).²⁵ Of note, we also detected a 4.2-Mb deletion involving *MED13L* in Patient 34
202 (Table S4 and Figure S2b). Further, a novel *PHIP* missense mutation (NM_017934.7:c.1156G>A,
203 p.Asp386Asn) was detected in Patient 56. *PHIP* haploinsufficiency causes dysmorphic CdLS-like
204 features, developmental delay, intellectual disability, and obesity.²⁶
205 In the remaining 21 undetermined families, NM_025146.4:c.93C>G, p.Tyr31* in *NAA50* (encoding
206 N-alpha-acetyltransferase 50) attracted our attention because it encodes a cohesin complex
207 component (see Discussion). *NAA50* variants have not previously been described.

208

209 **Clinical evaluation of CdLS patients using a new scoring system**

210 Of the 57 patients with CdLS, their clinical features were re-evaluated based on the clinical scoring
211 system reported by Kline *et al.*⁶ With this scoring system, clinical features of clinically suspected
212 CdLS are classified as cardinal (2 points each if presented) and suggestive (1 point each if
213 presented). Clinical scores ≥ 11 , 10 or 9, 8–4, and < 4 points, are classified as: classic CdLS, non-
214 classic CdLS, sufficiently suspected to warrant molecular testing for CdLS, and insufficient
215 indication for CdLS molecular testing, respectively. All 57 patients were classified using the above
216 clinical scoring system (Table S1 and Figure 3). Twenty-five patients were categorized as classic

217 CdLS, 17 patients as non-classic CdLS, and 15 patients as sufficiently suspected to warrant
218 molecular testing for CdLS. No patients were insufficient to indicate molecular testing. The
219 proportion of *NIPBL* variants was 60% (15/25), 35.3% (6/17), and 13.3% (2/15) in each class,
220 respectively. Ratios of *NIPBL* variants were compared between two of three classes, with a
221 significant difference recognized only between classic CdLS and sufficiently suspected to warrant
222 molecular testing for CdLS (χ^2 test, $p < 0.05$) (Figure 3). *NIPBL* variants in classic CdLS were more
223 frequent than sufficiently suspected to warrant molecular testing for CdLS.

224 Interestingly, Patient 53 with a *ZMYND11* frameshift variant showed classic CdLS (15 points) with
225 oligodactyly (Figure 2a–e). Therefore *ZMYND11* could be included as a CdLS or CdLS-like genes,
226 although *ZMYND11* variants have not been reported in CdLS. Patients 5 (SNV) and 34 (CNV) with
227 *MED13L* abnormality showed clinical scores of 8 and 9 points, respectively, and were consequently
228 classified as sufficiently suspected to warrant molecular testing for CdLS and non-classic CdLS
229 (Figure 2f–h, i–l). Patient 56 with a missense variant in *PHIP* showed CdLS-like features (6 points),
230 including synophrys, long curly eyelashes, anteverted nostrils, and depressed nasal bridge, although
231 obesity was retrospectively inconsistent with CdLS (Figure 2m–p). This clinical information is
232 summarized in Table S1.

233

234 **DISCUSSION**

235 Using WES, we identified pathogenic variants in 36 out of 57 (63.2%) patients with clinically
236 suspected CdLS. The diagnostic yield was comparatively higher than previous studies (40–60%) as
237 previous studies used panel or Sanger sequencing of only major CdLS genes.²⁷⁻³⁰ Advantages of
238 WES are clearly indicated here as CdLS and CdLS-like patients are genetically and clinically
239 heterogeneous. Using a large clinical exome sequencing cohort, a recent genotype-driven approach
240 of cohesinopathy also emphasized the utility of clinical exome sequencing to provide molecular
241 diagnoses for cohesinopathies with extensive genetic and phenotypic heterogeneity, as well as to
242 detecting mosaic variants in patients.¹² We detected no mosaicism variants in our patients, although
243 it may be difficult to detect extremely low prevalence mosaic variants by WES.

244 Based on recent clinical scores,⁶ *NIPBL* variants are more likely to be found in classic CdLS.
245 Moreover, we detected a *ZMYND11* frameshift variant, NM_006624.5:c.1438delG,
246 p.Asp480Thrfs*3 in Patient 53 with classic CdLS. *ZMYND11* (also known as BS69) contains a
247 tandem “reader” module of histone modifications, which recognizes and binds histone H3.3
248 trimethylated at Lys-36 (H3.3K36me3). Subsequently, this recruits histone demethylases, histone
249 deacetylases, and the SWI/SNF chromatin-remodeling complex to reset chromatin to a relatively
250 repressive state and prevent further transcription.^{31, 32} Except for *ZMYND11*, all pathogenic variants
251 in genes for diseases other than CdLS and CdLS-like (*MED13L* and *PHIP*) were detected in patients
252 with scores < 9.

253 We found two patients with *MED13L* abnormality and one patient with a *PHIP* variant. MED13 is a
254 subunit of the cyclin-dependent kinase 8 (CDK8) module comprised of reversible association of four
255 subunits: cyclin C, CDK8, mediator complex subunit (MED)12/MED12L, and MED13/MED13L. The
256 module binds the mediator complex to regulate its activity. The mediator complex bridges between
257 gene-specific activators bound to regulatory elements and general transcription machinery comprising
258 RNA polymerase II and general transcription factors.^{33,34} PHIP is a H3K4 methylation-binding protein
259 that interacts with chromatin modifications associated with promoters and transcriptional cis-
260 regulatory elements.³⁵ Interestingly, *ZMYND11*, *MED13L*, and *PHIP* are all core components of
261 transcriptional regulatory pathways. Recently, CdLS and CdLS-like disorders were reported not only
262 as cohesinopathies but also as “transcriptomopathies”.¹⁵ Actually, *AFF4*, *ANKRD11*, *ARID1B*, *BRD4*,
263 *EP300*, *KMT2A*, *SETD5*, and *TAF6* have been found in patients with several clinical features
264 overlapping with CdLS, and are related to epigenetic modification, chromatin remodeling, and
265 transcriptional regulation pathway^{8, 15, 36, 37} (Table S5). Interactive networks of 18 genes associated
266 with CdLS and CdLS-like features were analyzed using GeneMANIA (<https://genemania.org/>), which
267 covers physical interactions, pathways, and shared protein domains (Figure 4). As expected, genes
268 encoding cohesion complex and its regulatory factors (*NIBPL*, *SMC1A*, *SMC3*, *HDAC8*, *RAD21*, and
269 *ESPL1*) strongly interact with each other. *ZMYND11* and *PHIP* share protein domains with other genes
270 encoding histone modification factors and transcriptional regulation factors. *MED13L* shares a

271 common pathway with *EP300*, and is involved in regulation of RNA polymerase II. HIF1A is a
272 hypoxia inducible factor subunit that induces recruitment of CDK8-mediator complex and p300
273 (encoding EP300) for histone acetyltransferase to stimulate RNA polymerase II elongation.³⁸ These
274 functional links in three genes (*ZMYND11*, *PHIP*, and *MED13L*) may be related to CdLS-like features.
275 Patient 51 has a 14.1-Mb deletion at 9p24.3-p22.3 (involving 44 RefSeq genes) adjacent to a 571-kb
276 duplication at 9p22.3, containing four genes (Figure S2c). Critical genes of 9p deletion syndrome
277 include *DMRT* (*DMRT1*, *DMRT2*, and *DMRT3* cluster) for gonadal dysgenesis from complete sex
278 reversal to milder phenotypes in 46,XY patients,³⁹ *FREMI* for craniosynostosis including
279 trigonocephaly,⁴⁰ and *DOCK8*, *KANK1*, *SLCIA1*, and *GLDC* for developmental delay and
280 neurological disorders.⁴¹ Trigonocephaly is one of the major features of 9p deletion syndrome, but
281 absent in our patient. Trigonocephaly was previously mapped to a critical 4.7-Mb region at 9p22.2-
282 p23, including *FREMI* and *CER1*.⁴² Interestingly, our patient has a duplication of this critical region,
283 and instead of trigonocephaly, exhibited delayed closure of the anterior fontanelle at 3 years of age
284 Thus, it is conceivable that *FREMI* and/or *CER1* are potentially dosage sensitive genes related to
285 cranial bone development and closure. In addition, *SMARCA2* was included in the deletion region.
286 *SMARCA2* is a known causative gene for Nicolaides–Baraitser syndrome (MIM #601358), which shares
287 several CdLS features.⁴³ To date, 78 variants are registered in the Human Gene Mutation Database (HGMD)
288 V.2019.1, but no truncating variants. *SMARCA2* variants are predicted to act in a dominant-negative or

289 gain-of-function manner rather than haploinsufficiency. Indeed, it has been suggested that *SMARCA2* might
290 not be a critical gene for 9p deletion syndrome.

291 Patient 52 has a 773.8-kb deletion at 9q34.3, which contains 14 genes including *EHMT1*. Intragenic
292 *EHMT1* variants or submicroscopic 9q34.3 deletion causes Kleefstra syndrome with distinct facial
293 features, hypotonia, developmental delay, and intellectual disability.⁴⁴ *EHMT1* encodes a histone H3
294 Lys-9 methyltransferase and is consequently involved in chromatin remodeling.⁴⁵ Similar to patients
295 with CdLS, our patient showed dysmorphic features, including synophrys, long curly eyelashes, and
296 depressed nasal bridge, but no limb abnormalities (Figure 2u–w). Clinical score was 5 points,
297 suggesting that the patient is likely compatible with Kleefstra syndrome rather than CdLS. Nonetheless,
298 it is sometimes difficult to clearly differentiate these two disorders.

299 In 21 undetermined families, a *de novo* nonsense variant (NM_025146.4:c.93C>G, p.Tyr319*) was
300 detected in *NAA50* in Patient 19 with classic CdLS features (12 points). The variant was confirmed by
301 Sanger sequencing. This variant was not registered in control population databases (ExAC and
302 gnomAD). According to ExAC, probability of loss-of-function intolerance (pLI) score of 0.88 suggest
303 intolerance to loss-of-function variant. To date, no variants are registered in HGMD V.2019.1. *NAA50*
304 encodes a N-terminal acetyltransferase required for chromosome segregation during mitosis. It has
305 been reported that *NAA50* is required for sister chromatid cohesion during *Drosophila* wing
306 development, and most likely regulates correct interaction between the cohesin subunits, RAD21 and

307 SMC3.⁴⁶ These findings support that *NAA50* truncation variants may cause the candidate variants of
308 CdLS. Further studies of *NAA50* variants in patients with CdLS are necessary.

309 In conclusion, we have achieved a high genetic diagnosis rate of 63.2% by WES in patients with
310 clinically diagnosed CdLS. Moreover, we have newly detected *ZMYND11*, *MED13L*, and *PHIP*
311 variants potentially linked to CdLS or CdLS-like through abnormality of transcriptional regulation
312 together with *NAA50* variant.

313

314 **Acknowledgments**

315 We would like to thank the patients and their families, and especially the Brazilian Association of
316 Cornelia de Lange Syndrome (CdLS Brazil) for participating in this study. We also thank N. Watanabe,
317 T. Miyama, M. Sato, S. Sugimoto, and K. Takabe for their technical assistance. This work was
318 supported by Japan Agency for Medical Research and Development (AMED) under grant numbers
319 JP18ek0109280, JP18dm0107090, JP18ek0109301, JP18ek0109348, and JP18kk0205001; by Japan
320 Society for the Promotion of Science (JSPS) KAKENHI under grant numbers JP17H01539,
321 JP16H05357, JP16H06254, JP17K16132, JP17K10080, JP17K15630, and JP17H06994; by the
322 Ministry of Health, Labour, and Welfare; and by the Takeda Science Foundation. We thank Sarah
323 Williams, PhD, from Edanz Group (www.edanzediting.com) for editing a draft of this manuscript.

324

325 **Supplementary information** is available at Journal of human genetics's website.

326 **References**

327

- 328 1. Nizon, M., Henry, M., Michot, C., Baumann, C., Bazin, A., Bessieres, B. et al. A
329 series of 38 novel germline and somatic mutations of NIPBL in Cornelia de Lange
330 syndrome. *Clinical Genetics*. 2016;89:584–89.
- 331 2. Mannini, L., Cucco, F., Quarantotti, V., Krantz, I.D., Musio, A. Mutation spectrum
332 and genotype-phenotype correlation in Cornelia de Lange syndrome. *Human*
333 *Mutation*. 2013;34:1589–96.
- 334 3. Bhuiyan, Z.A., Klein, M., Hammond, P., van Haeringen, A., Mannens, M.M., Van
335 Berckelaer-Onnes, I. et al. Genotype-phenotype correlations of 39 patients with
336 Cornelia De Lange syndrome: the Dutch experience. *Journal of Medical Genetics*.
337 2006;43:568–75.
- 338 4. Bedoukian, E., Copenheaver, D., Bale, S., Deardorff, M. Bohring-Opitz syndrome
339 caused by an ASXL1 mutation inherited from a germline mosaic mother. *American*
340 *Journal of Medical Genetics. Part A*. 2018;176:1249–52.
- 341 5. McInerney-Leo, A.M., Harris, J.E., Gattas, M., Peach, E.E., Sinnott, S., Dudding-
342 Byth, T. et al. Fryns Syndrome Associated with Recessive Mutations in PIGN in two
343 Separate Families. *Human Mutation*. 2016;37:695–702.
- 344 6. Kline, A.D., Moss, J.F., Selicorni, A., Bisgaard, A.M., Deardorff, M.A., Gillett, P.M. et
345 al. Diagnosis and management of Cornelia de Lange syndrome: first international
346 consensus statement. *Nature Reviews Genetics*. 2018;19:649–66.
- 347 7. Parenti, I., Teresa-Rodrigo, M.E., Pozojevic, J., Ruiz Gil, S., Bader, I., Braunholz, D.
348 et al. Mutations in chromatin regulators functionally link Cornelia de Lange
349 syndrome and clinically overlapping phenotypes. *Human Genetics*. 2017;136:307–
350 20.
- 351 8. Olley, G., Ansari, M., Bengani, H., Grimes, G.R., Rhodes, J., von Kriegsheim, A. et
352 al. BRD4 interacts with NIPBL and BRD4 is mutated in a Cornelia de Lange-like
353 syndrome. *Nature Genetics*. 2018;50:329–32.
- 354 9. Ansari, M., Poke, G., Ferry, Q., Williamson, K., Aldridge, R., Meynert, A.M. et al.
355 Genetic heterogeneity in Cornelia de Lange syndrome (CdLS) and CdLS-like
356 phenotypes with observed and predicted levels of mosaicism. *Journal of Medical*
357 *Genetics*. 2014;51:659–68.
- 358 10. Yavarna, T., Al-Dewik, N., Al-Mureikhi, M., Ali, R., Al-Mesaifri, F., Mahmoud, L. et
359 al. High diagnostic yield of clinical exome sequencing in Middle Eastern patients
360 with Mendelian disorders. *Human Genetics*. 2015;134:967–80.
- 361 11. Muto, A., Schilling, T.F. Zebrafish as a Model to Study Cohesin and

- 362 Cohesinopathies. In: *Methods in Molecular Biology*. Clifton, N.J; 2017. p. 177–196.
- 363 12. Yuan, B., Neira, J., Pehlivan, D., Santiago-Sim, T., Song, X., Rosenfeld, J. et al.
- 364 Clinical exome sequencing reveals locus heterogeneity and phenotypic variability of
- 365 cohesinopathies. *Genetics in Medicine: Official Journal of the American College of*
- 366 *Medical Genetics*. 2019;3:663-75.
- 367 13. Izumi, K., Nakato, R., Zhang, Z., Edmondson, A.C., Noon, S., Dulik, M.C. et al.
- 368 Germline gain-of-function mutations in *AFF4* cause a developmental syndrome
- 369 functionally linking the super elongation complex and cohesin. *Nature Genetics*.
- 370 2015;47:338–44.
- 371 14. Woods, S.A., Robinson, H.B., Kohler, L.J., Agamanolis, D., Sterbenz, G., Khalifa, M.
- 372 Exome sequencing identifies a novel *EP300* frame shift mutation in a patient with
- 373 features that overlap Cornelia de Lange syndrome. *American Journal of Medical*
- 374 *Genetics. Part A*. 2014;164a:251–58.
- 375 15. Yuan, B., Pehlivan, D., Karaca, E., Patel, N., Charng, W.L., Gambin, T. et al. Global
- 376 transcriptional disturbances underlie Cornelia de Lange syndrome and related
- 377 phenotypes. *The Journal of Clinical Investigation*. 2015;125:636–51.
- 378 16. Fromer, M., Moran, J.L., Chambert, K., Banks, E., Bergen, S.E., Ruderfer, D.M. et
- 379 al. Discovery and statistical genotyping of copy-number variation from whole-exome
- 380 sequencing depth. *American Journal of Human Genetics*. 2012;91:597–607.
- 381 17. Nord, A.S., Lee, M., King, M.C., Walsh, T. Accurate and exact CNV identification
- 382 from targeted high-throughput sequence data. *BMC Genomics*. 2011;12:184.
- 383 18. Richards, S., Aziz, N., Bale, S., Bick, D., Das, S., Gastier-Foster, J. et al. Standards
- 384 and guidelines for the interpretation of sequence variants: a joint consensus
- 385 recommendation of the American College of Medical Genetics and Genomics and the
- 386 Association for Molecular Pathology. *Genetics in medicine : official journal of the*
- 387 *American College of Medical Genetics*. 2015;17:405-24.
- 388 19. Selicorni, A., Russo, S., Gervasini, C., Castronovo, P., Milani, D., Cavalleri, F. et al.
- 389 Clinical score of 62 Italian patients with Cornelia de Lange syndrome and
- 390 correlations with the presence and type of *NIPBL* mutation. *Clinical Genetics*.
- 391 2007;72:98–108.
- 392 20. Gillis, L.A., McCallum, J., Kaur, M., DeScipio, C., Yaeger, D., Mariani, A. et al.
- 393 *NIPBL* mutational analysis in 120 individuals with Cornelia de Lange syndrome
- 394 and evaluation of genotype-phenotype correlations. *American Journal of Human*
- 395 *Genetics*. 2004;75:610–23.
- 396 21. Teresa-Rodrigo, M.E., Eckhold, J., Puisac, B., Pozojevic, J., Parenti, I., Baquero-
- 397 Montoya, C. et al. Identification and Functional Characterization of Two Intronic

- 398 NIPBL Mutations in Two Patients with Cornelia de Lange Syndrome. *BioMed*
399 *Research International*. 2016;8742939.
- 400 22. Cheng, Y.W., Tan, C.A., Minor, A., Arndt, K., Wysinger, L., Grange, D.K. et al. Copy
401 number analysis of NIPBL in a cohort of 510 patients reveals rare copy number
402 variants and a mosaic deletion. *Molecular Genetics & Genomic Medicine*.
403 2014;2:115–23.
- 404 23. Tumiene, B., Ciuladaite, Z., Preiksaitiene, E., Mameniskiene, R., Utkus, A.,
405 Kucinkas, V. Phenotype comparison confirms ZMYND11 as a critical gene for
406 10p15.3 microdeletion syndrome. *Journal of Applied Genetics*. 2017;58:467–74.
- 407 24. Smol, T., Petit, F., Piton, A., Keren, B., Sanlaville, D., Afenjar, A. et al. MED13L-
408 related intellectual disability: involvement of missense variants and delineation of
409 the phenotype. *Neurogenetics*. 2018;19:93–103.
- 410 25. Bowling, K.M., Thompson, M.L., Amaral, M.D., Finnila, C.R., Hiatt, S.M., Engel,
411 K.L. et al. Genomic diagnosis for children with intellectual disability and/or
412 developmental delay. *Genome Medicine*. 2017;9:43.
- 413 26. Jansen, S., Hoischen, A., Coe, B.P., Carvill, G.L., Van Esch, H., Bosch, D.G.M. et al.
414 A genotype-first approach identifies an intellectual disability-overweight syndrome
415 caused by PHIP haploinsufficiency. *European Journal of Human Genetics*.
416 2018;26:54–63.
- 417 27. Mariani, M., Decimi, V., Bettini, L.R., Maitz, S., Gervasini, C., Masciadri, M. et al.
418 Adolescents and adults affected by Cornelia de Lange syndrome: A report of 73
419 Italian patients. *American Journal of Medical Genetics. Part C, Seminars in*
420 *Medical Genetics*. 2016;172:206–13.
- 421 28. Marchisio, P., Selicorni, A., Bianchini, S., Milani, D., Baggi, E., Cerutti, M. et al.
422 Audiological findings, genotype and clinical severity score in Cornelia de Lange
423 syndrome. *International Journal of Pediatric Otorhinolaryngology*. 2014;78:1045–
424 48.
- 425 29. Hei, M., Gao, X., Wu, L. Clinical and genetic study of 20 patients from China with
426 Cornelia de Lange syndrome. *BMC Pediatrics*. 2018;18:64.
- 427 30. Mehta, D., Vergano, S.A., Deardorff, M., Aggarwal, S., Barot, A., Johnson, D.M. et
428 al. Characterization of limb differences in children with Cornelia de Lange
429 Syndrome. *American journal of medical genetics. Part C, Seminars in Medical*
430 *Genetics*. 2016;172:155–62.
- 431 31. Wen, H., Li, Y., Li, H., Shi, X. ZMYND11: an H3.3-specific reader of H3K36me3.
432 *Cell Cycle*. 2014;13:2153–54.
- 433 32. Wen, H., Li, Y., Xi, Y., Jiang, S., Stratton, S., Peng, D. et al. ZMYND11 links histone

- 434 H3.3K36me3 to transcription elongation and tumour suppression. *Nature*.
435 2014;508:263–68.
- 436 33. Utami, K.H., Winata, C.L., Hillmer, A.M., Aksoy, I., Long, H.T., Liany, H. et al.
437 Impaired development of neural-crest cell-derived organs and intellectual disability
438 caused by MED13L haploinsufficiency. *Human Mutation*. 2014;35:1311–20.
- 439 34. Miao, Y.L., Gambini, A., Zhang, Y., Padilla-Banks, E., Jefferson, W.N., Bernhardt,
440 M.L. et al. Mediator complex component MED13 regulates zygotic genome
441 activation and is required for postimplantation development in the mouse. *Biology*
442 *of Reproduction*. 2018;98:449–64.
- 443 35. Morgan, M.A.J., Rickels, R.A., Collings, C.K., He, X., Cao, K., Herz, H.M. et al. A
444 cryptic Tudor domain links BRWD2/PHIP to COMPASS-mediated histone H3K4
445 methylation. *Genes & Development*. 2017;31:2003–14.
- 446 36. Izumi, K. Disorders of Transcriptional Regulation: An Emerging Category of
447 Multiple Malformation Syndromes. *Molecular Syndromology*. 2016;7:262–73.
- 448 37. Ka, M., Kim, W.Y. ANKRD11 associated with intellectual disability and autism
449 regulates dendrite differentiation via the BDNF/TrkB signaling pathway.
450 *Neurobiology of Disease*. 2018;111:138–52.
- 451 38. Galbraith, M.D., Allen, M.A., Bensard, C.L., Wang, X., Schwinn, M.K., Qin, B. et al.
452 HIF1A employs CDK8-mediator to stimulate RNAPII elongation in response to
453 hypoxia. *Cell*. 2013;153:1327-39.
- 454 39. Onesimo, R., Orteschi, D., Scalzone, M., Rossodivita, A., Nanni, L., Zannoni, G.F. et
455 al. Chromosome 9p deletion syndrome and sex reversal: novel findings and
456 redefinition of the critically deleted regions. *American Journal of Medical Genetics*.
457 *Part A*. 2012;158a:2266–71.
- 458 40. Vissers, L.E., Cox, T.C., Maga, A.M., Short, K.M., Wiradjaja, F., Janssen, I.M. et al.
459 Heterozygous mutations of FREM1 are associated with an increased risk of isolated
460 metopic craniosynostosis in humans and mice. *PLoS Genetics*. 2011;7:e1002278.
- 461 41. Recalcati, M.P., Bellini, M., Norsa, L., Ballarati, L., Caselli, R., Russo, S. et al.
462 Complex rearrangement involving 9p deletion and duplication in a syndromic
463 patient: genotype/phenotype correlation and review of the literature. *Gene*.
464 2012;502:40–5.
- 465 42. Kawara, H., Yamamoto, T., Harada, N., Yoshiura, K., Niikawa, N., Nishimura, A. et
466 al. Narrowing candidate region for monosomy 9p syndrome to a 4.7-Mb segment at
467 9p22.2-p23. *American Journal of Medical Genetics. Part A*. 2006;140:373–77.
- 468 43. Sousa, S.B., Hennekam, R.C. Phenotype and genotype in Nicolaides-Baraitser
469 syndrome. *American Journal of Medical Genetics. Part C, Seminars in Medical*

470 Genetics. 2014;166c:302–14.

471 44. Willemsen, M.H., Vulto-van Silfhout, A.T., Nillesen, W.M., Wissink-Lindhout, W.M.,
472 van Bokhoven, H., Philip, N. et al. Update on Kleefstra Syndrome. *Molecular*
473 *Syndromology*. 2012;2:202–12.

474 45. Iacono, G., Dubos, A., Meziane, H., Benevento, M., Habibi, E., Mandoli, A. et al.
475 Increased H3K9 methylation and impaired expression of Protocadherins are
476 associated with the cognitive dysfunctions of the Kleefstra syndrome. *Nucleic Acids*
477 *Research*. 2018;46:4950–65.

478 46. Ribeiro, A.L., Silva, R.D., Foyen, H., Tiago, M.N., Rathore, O.S., Arnesen, T. et al.
479 Naa50/San-dependent N-terminal acetylation of Scc1 is potentially important for
480 sister chromatid cohesion. *Scientific Reports*. 2016;6:39118.

481 47. Gillis, L.A., McCallum, J., Kaur, M., DeScipio, C., Yaeger, D., Mariani, A. et al.
482 NIPBL mutational analysis in 120 individuals with Cornelia de Lange syndrome
483 and evaluation of genotype-phenotype correlations. *American journal of human*
484 *genetics*. 2004;75:610-23.

485 48. Oliveira, J., Dias, C., Redeker, E., Costa, E., Silva, J., Reis Lima, M. et al.
486 Development of NIPBL locus-specific database using LOVD: from novel mutations
487 to further genotype-phenotype correlations in Cornelia de Lange Syndrome. *Human*
488 *mutation*. 2010;31:1216-22.

489 49. Deardorff, M.A., Kaur, M., Yaeger, D., Rampuria, A., Korolev, S., Pie, J. et al.
490 Mutations in cohesin complex members SMC3 and SMC1A cause a mild variant of
491 cornelia de Lange syndrome with predominant mental retardation. *American*
492 *journal of human genetics*. 2007;80:485-94.

493

494 **Titles and legends to figures**

495 **Figure 1. Flowchart of this study.**

496 All the 57 patients with clinically suspected CdLS were analyzed by whole exome sequencing
497 (WES). Twenty-nine patients had pathogenic single nucleotide variants (SNVs) in two CdLS genes
498 (*NIPBL* and *SMC1A*) and four CdLS-like genes (*ANKRD11*, *EP300*, *KMT2A*, and *SETD5*). WES-
499 based copy number variation (CNV) analysis in patients with no causative SNVs identified
500 pathogenic CNVs in four patients. The remaining 24 patients with neither pathogenic SNVs nor
501 CNVs were subjected to trio-based analysis, except for two cases whose parental samples were
502 unavailable. Three causative variants were identified in *ZMYND11*, *MED13L*, and *PHIP*. Diagnostic
503 yield was 63.2 % (36/57) when all 32 SNVs (32/57 [56.1%]) and four CNVs (4/57 [7.0%]) were
504 included. A novel candidate variant was detected in *NAA50*.

505

506 **Figure 2. Clinical photographs of individuals with *ZMYND11*, *MED13L*, and *PHIP***

507 **abnormalities.** (a–e) Photos of Patient 53 with a *ZMYND11* frameshift mutation. (a, b) Facial
508 features include microcephaly, synophrys, highly arched eyebrows, long curly eyelashes, low set
509 ears, anteverted nasal nostrilis, long philtrum, thin upper lip, downturned corners of the mouth, and
510 micrognathia. (c) Note left hand oligodactyly (only one finger). (d, e) Right hand and bilateral feet.
511 Right hand shows abnormal palmer crease. Feet show no abnormalities. (f–h) Facial photos of

512 Patient 5 with a *MED13L* missense mutation at (f) 3 months and (g) 18 years. (h) Broad forehead,
513 synophrys, long curly eyelashes, low set ears, anteverted nasal bridge, and full cheeks are seen at 23
514 years. (i–l) Clinical features of Patient 34 with a 4.2-Mb deletion involving *MED13L*. (i) Note
515 synophrys, arched eyebrows, upslanting palpebral fissures, long curly eyelashes, low set ears,
516 anteverted nasal bridge, and bulbous nasal tip. (j) Hirsutism in the back. (k, l) Bilateral hands and
517 feet. Hands show clinodactyly of the fifth finger. Feet show no abnormalities. (m–p) Photos of
518 Patient 56 with a *PHIP* missense mutation. (m) Facial features include macrocephaly, synophrys,
519 long curly eyelashes, anteverted nasal nostrilis, depressed nasal bridge, and short neck. (n) Full
520 whole body view with obesity at 11 years (weight, 82.5 kg [> 95 percentile]; height, 157.5 cm [> 95
521 percentile]; occipital frontal circumference, 58 cm [> 98 percentile]). (o, p) Hands and feet were
522 normal. (q–t) Photos of Patient 51 with a 4.1-Mb deletion at 9p24.3-p22.3 adjacent to a 571-kb
523 duplication at 9p22.3. (q, r) Facial features include synophrys, upslanting palpebral fissures,
524 anteverted nostrilis, and long philtrum. (s, t) Hands were normal. (u–w) Phenotype of Patient 52 with
525 a 773.8-kb deletion at 9q34.3. (u) Facial features include synophrys, long curly eyelashes, and
526 depressed nasal bridge. (v, w) Hands and feet were normal.

527

528 **Figure 3. Classification of 57 CdLS patients by clinical score.** All patients were classified based
529 on clinical score. Scores of ≥ 11 , 10 or 9, 8–4, and < 4 enabled categorization of four classes: classic

530 CdLS, non-classic CdLS, sufficiently suspected to warrant molecular testing for CdLS indicated, and
531 insufficient to indicate molecular testing for CdLS. The 57 patients were classified to classic CdLS
532 ($N = 25$), non-classic CdLS ($N = 17$), and sufficiently suspected to warrant molecular testing for
533 CdLS indicated ($N = 15$). The number of individuals with variants are indicated in rows of genes.

534

535 **Figure 4. Schematic presentation of interacting networks of mutated genes in CdLS and CdLS-**
536 **like.** Interactive gene networks of mutated genes with CdLS and CdLS-like features. Three networks
537 are highlighted using GeneMANIA (<https://genemania.org/>), based on physical interactions (red line),
538 connecting pathways (blue line), and shared protein domains (green line).

539

540

Figure 1

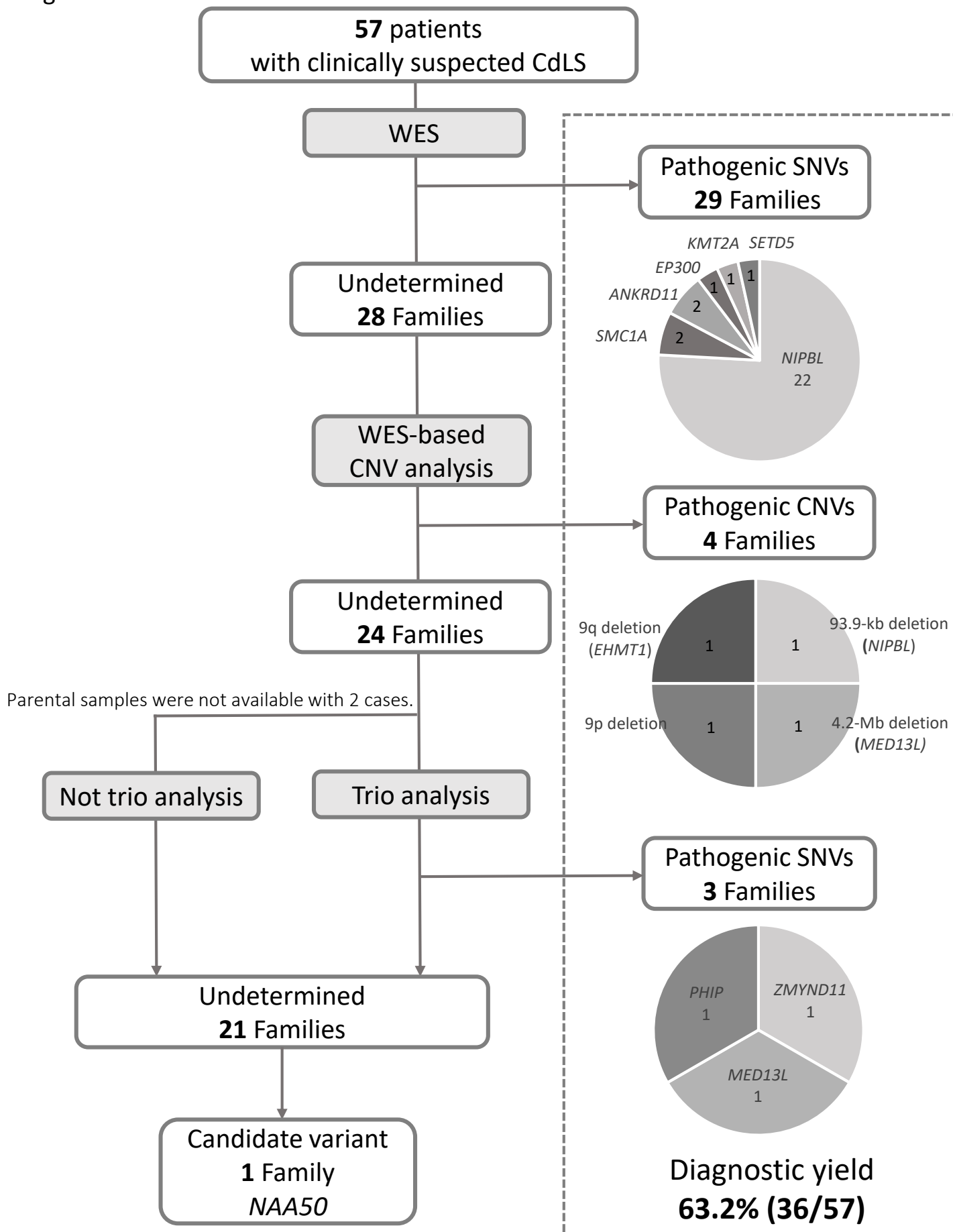


Figure 2

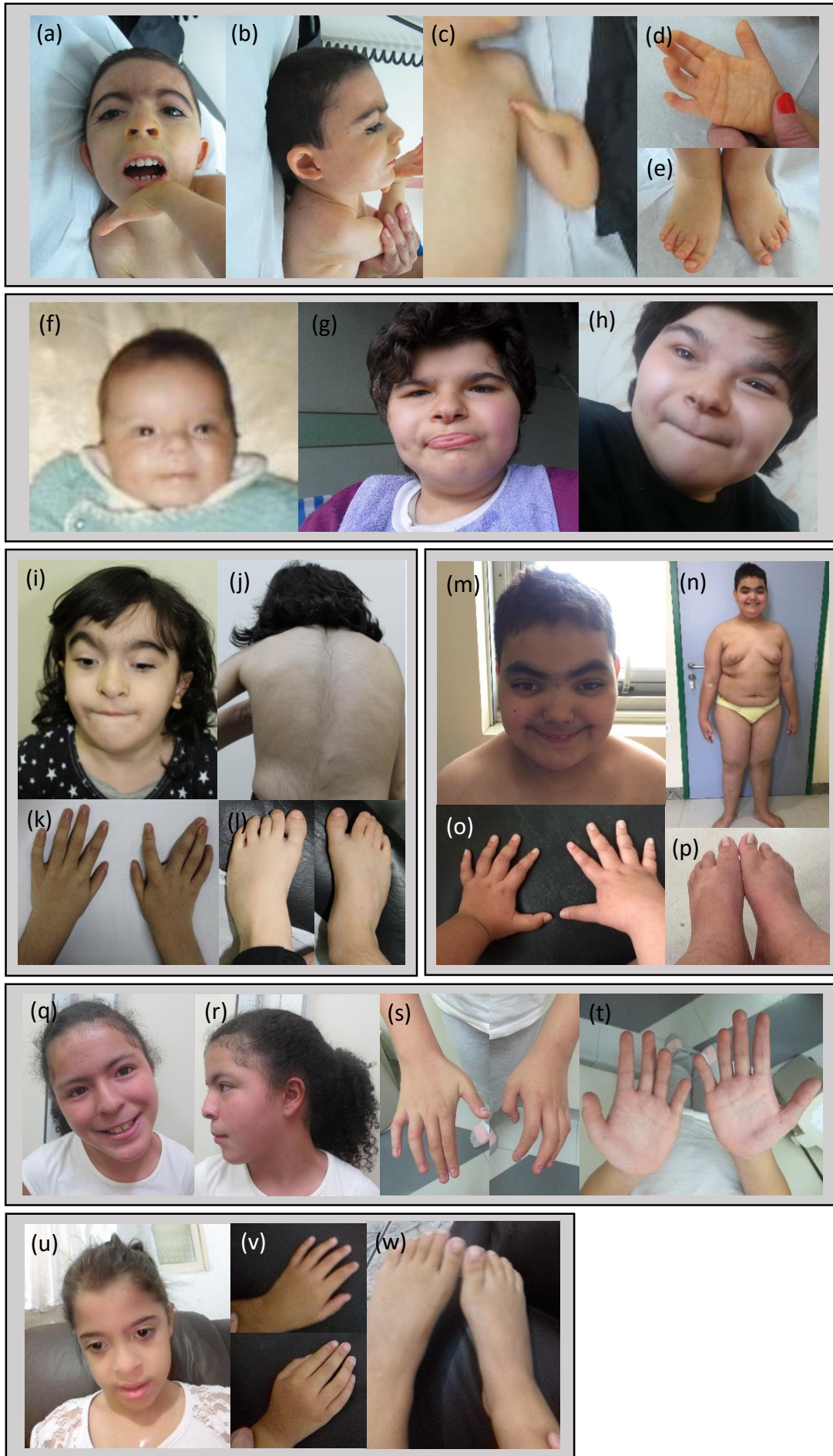
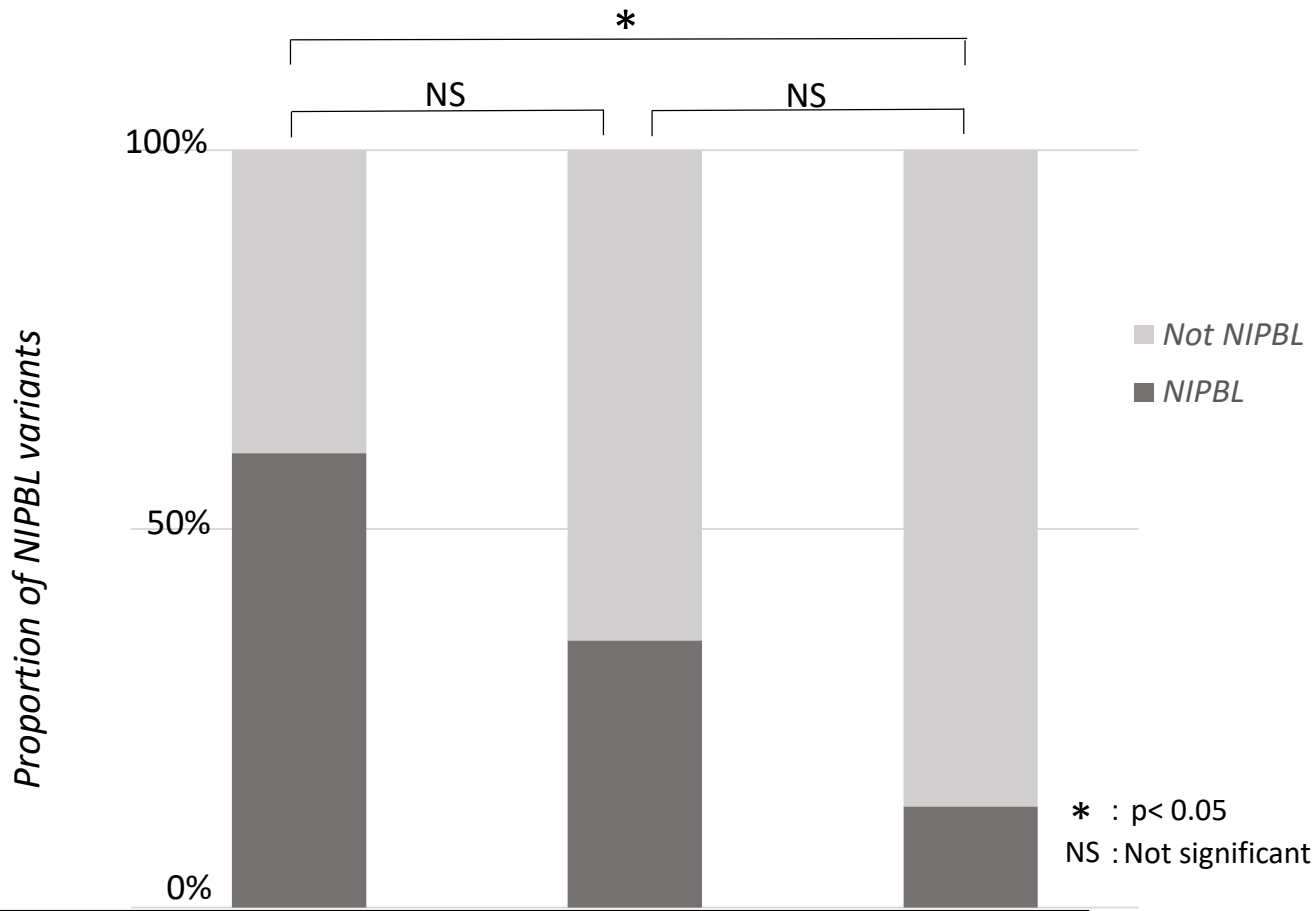


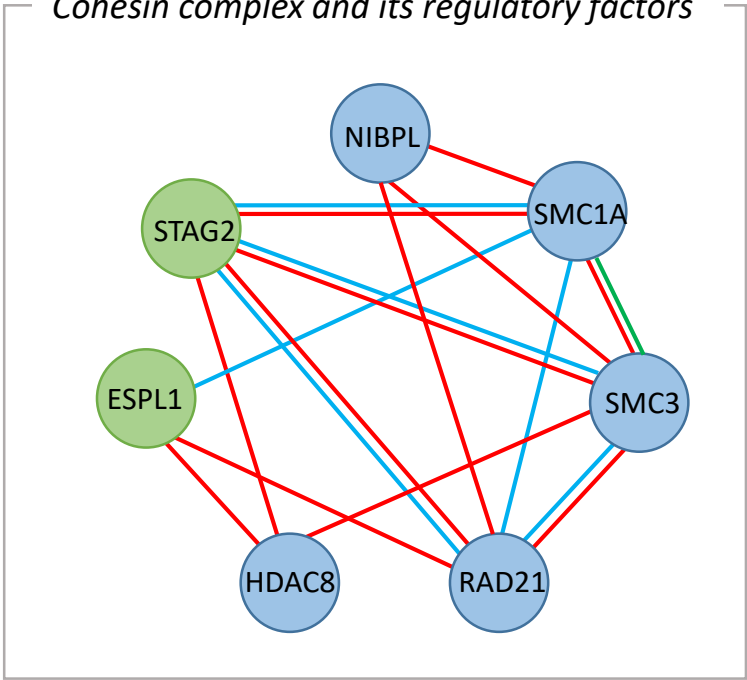
Figure 3



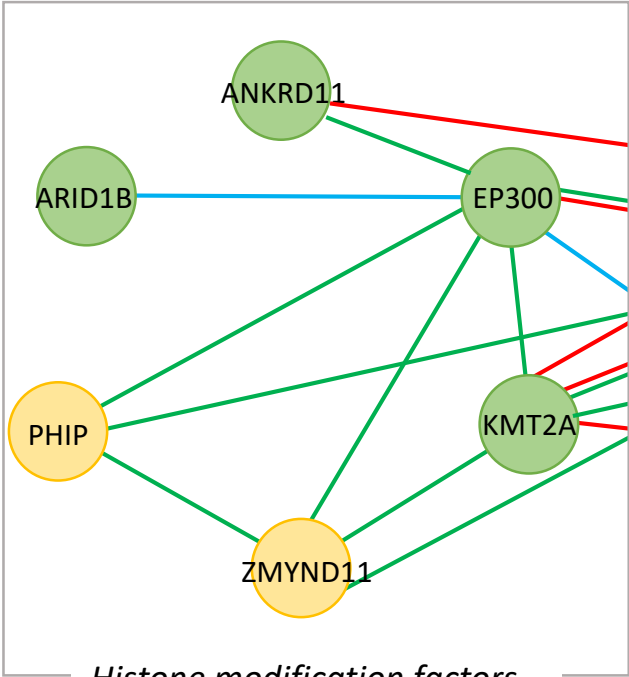
	Classic CdLS (Score \geq 11)	Non-classic CdLS (Score 10 or 9)	Molecular test (Score 8-4)
<i>NIPBL</i>	14 (SNV) 1 (CNV)	6	2
<i>SMC1A</i>	1	0	1
<i>ANKRD11</i>	0	1	1
<i>EP300</i>	0	1	0
<i>KMT2A</i>	0	0	1
<i>SETD5</i>	0	1	0
<i>ZMYND11</i>	1	0	0
<i>MED13L</i>	0	1 (CNV)	1
<i>PHIP</i>	0	0	1
CNV	0	0	2
Undetermined	8	7	6
Total	25	17	15

Figure 4

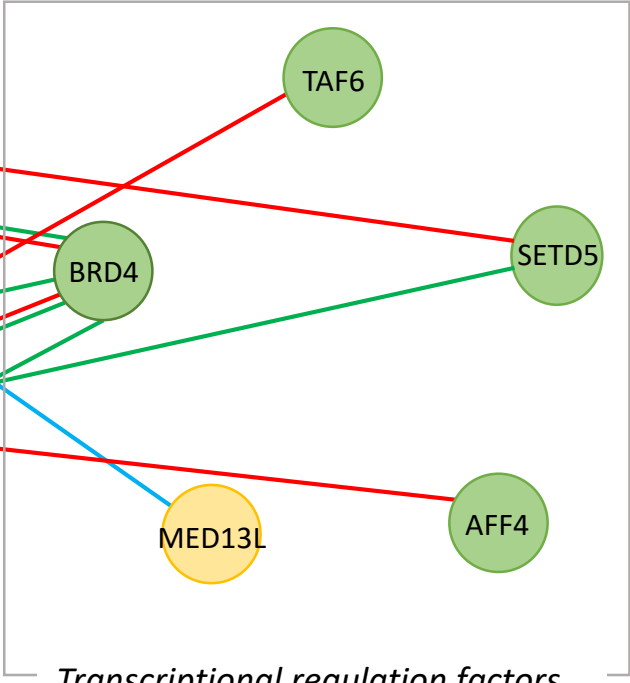
Cohesin complex and its regulatory factors



- CdLS genes
- CdLS-like genes
- Genes associated with diseases other than CdLS and CdLS-like
- Physical interactions
- Pathways
- Shared domains



Histone modification factors

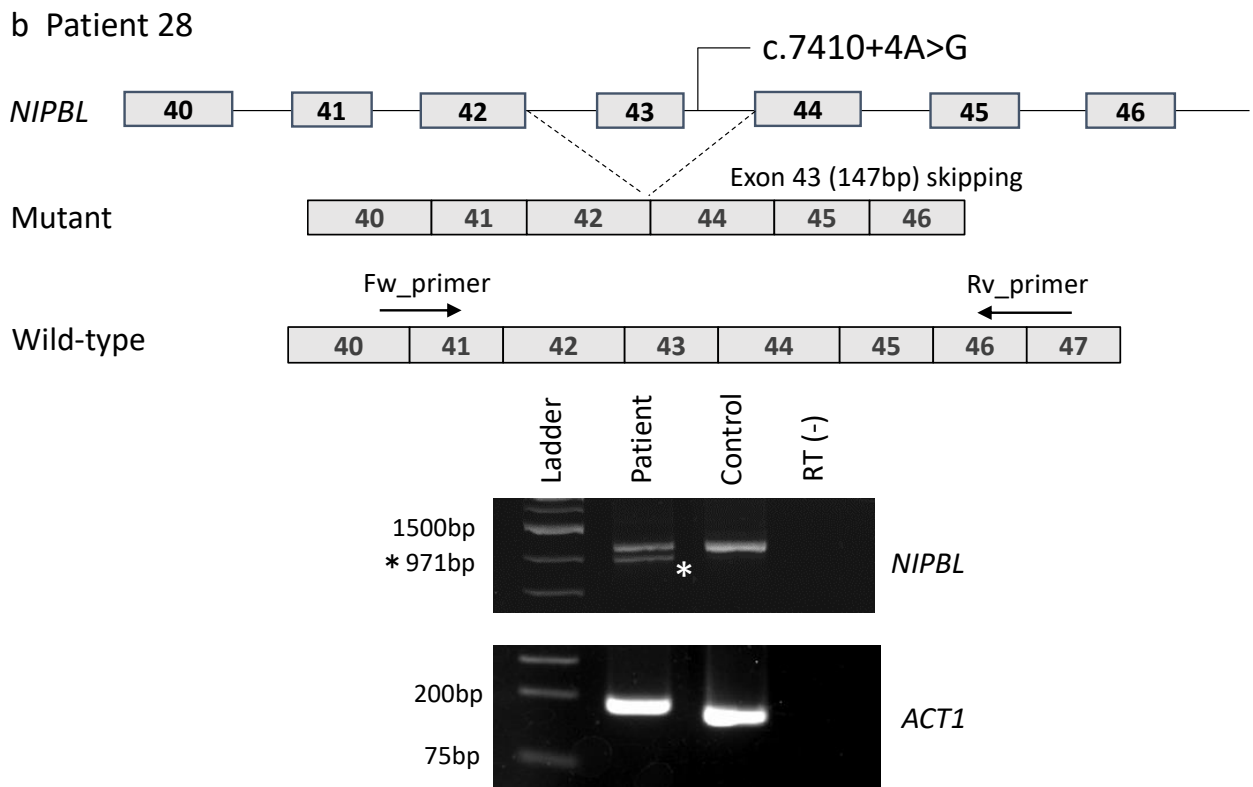
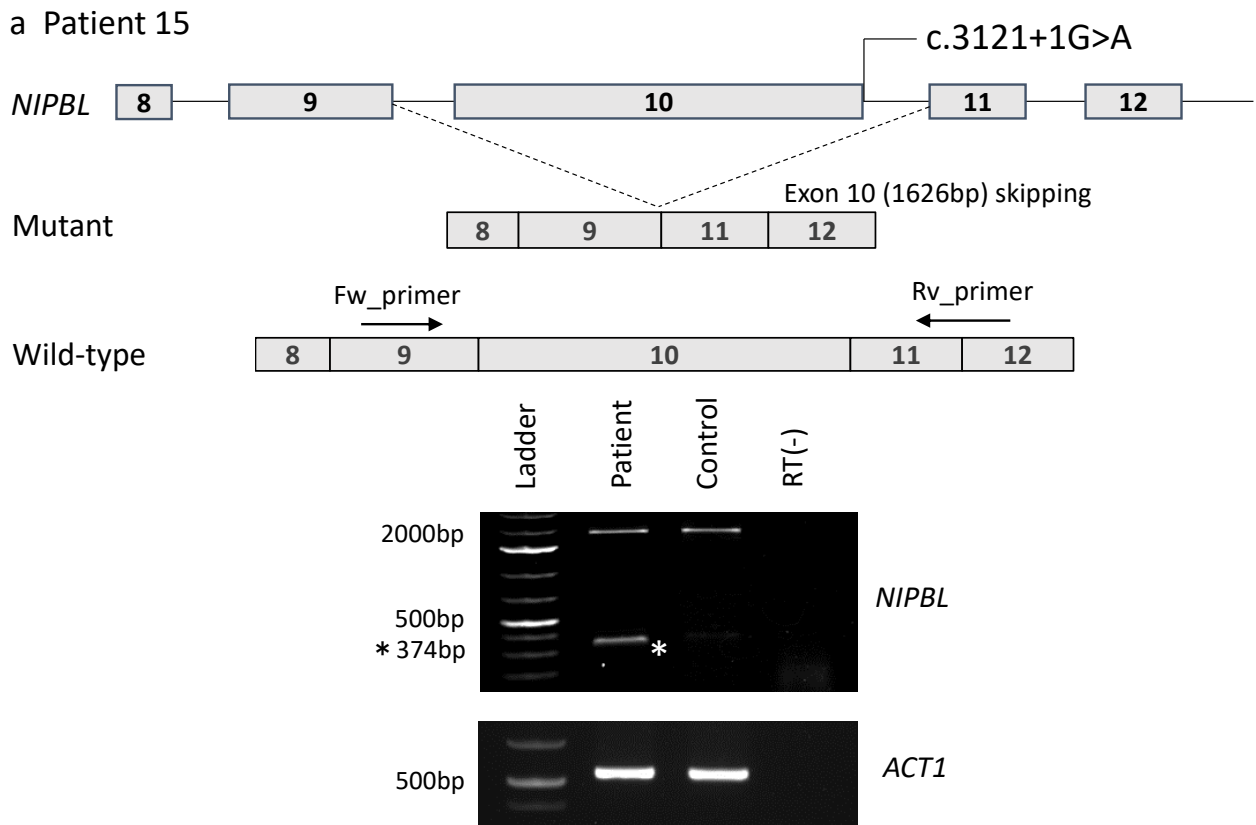


Transcriptional regulation factors

Gene	HGMD accession	Patient	Variant type	Mutation (hg 19)	Protein	Inheritance	Prediction scores			Control database			Novelty	
							SIFT	Polyphen2	Mutation taster	ESP6500	ExAC	575 in-house		
NIPBL	NM_0133433.3	2	missense	c.6893G>A	p.Arg2298His	de novo	D	D	D	-	-	0	Reported [47]	
		3	nonsense	c.6179dup	p.His2060Glnfs*4	de novo	-	-	-	-	-	0	Novel	
		4	missense	c.7699T>G	p.Tyr2567Asp	de novo	D	D	D	-	-	0	Novel	
		7	missense	c.5595G>T	p.Arg1865Ser	unavailable	D	D	D	-	-	0	Novel	
		8	missense	c.6620T>C	p.Met2207Thr	de novo	D	D	D	-	-	0	Novel	
		9	CNV	93.9-Kb deletion	-	not confirmed	-	-	D	-	-	-	-	Novel
		10	frameshift	c.5174delA	p.Lys1725Serfs*17	unavailable	-	-	D	-	-	0	Novel	
		13	frameshift	c.2479_2480delAG	p.Arg827Glyfs*2	de novo	-	-	D	-	-	0	Reported [47]	
		15	splicing	c.3121+1G>A	-	de novo	-	-	-	-	-	0	Reported [19]	
		17	frameshift	c.1903_1904insA	p.Ser635Tyrfs*3	de novo	-	-	D	-	-	0	Novel	
		25	frameshift	c.5030_5031del	p.Ile1677Serfs*21	de novo	-	-	D	-	-	0	Novel	
		28	splicing	c.7410+4A>G	-	de novo	-	-	-	-	-	0	Reported [20]	
		31	in-frame deletion	c.6653_6655del	p.Asn2218del	de novo	-	-	D	-	-	0	Novel	
		36	nonsense	c.5509C>T	p.Arg1837*	de novo	-	-	D	-	-	0	Novel	
		38	nonsense	c.826C>T	p.Gln276*	de novo	-	-	D	-	-	0	Reported [48]	
		39	nonsense	c.190C>T	p.Gln64*	de novo	-	-	D	-	-	0	Reported [9]	
		41	missense	c.6343G>T	p.Gln2115Cys	de novo	D	D	D	-	-	0	Novel	
		45	missense	c.6027G>C	p.Leu2009Phe	de novo	D	D	D	-	-	0	Novel	
		48	frameshift	c.8325_8326delinsT	p.Lys2775Asnfs*4	de novo	-	-	D	-	-	0	Novel	
		49	missense	c.6448C>G	p.Leu2150Val	de novo	T	D	D	-	-	0	Novel	
50	missense	c.6893G>A	p.Arg2298His	de novo	D	D	D	-	-	0	Reported [47]			
54	splicing	c.5329-15A>G	-	de novo	-	-	-	-	-	0	Reported [21]			
55	missense	c.7079G>T	p.Gly2360Val	de novo	D	D	D	-	-	0	Novel			
SMC1A	NM_006306.3	11	missense	c.1152C>G	p.Lys362Asn	de novo	D	D	D	-	-	0	Novel	
		42	missense	c.1487G>A	p.Arg496His	de novo	D	D	D	-	-	0	Reported [49]	
ANKRD11	NM_013275.5	21	frameshift	c.3255_3256del	p.Lys1086Glnfs*15	de novo	-	-	D	-	-	0	Novel	
		43	nonsense	c.5434C>T	p.Gln1812*	de novo	-	-	D	-	-	0	Novel	
EP300	NM_001429.3	6	in-frame deletion	c.7014_7028del	p.His2338_Pro2342del	unavailable	-	-	P	-	-	0	Novel	
KMT2A	NM_001197104.1	27	nonsense	c.3592C>T	p.Gln1198*	de novo	-	-	D	-	-	0	Novel	
SETD5	NM_001080517.2	1	nonsense	c.1852C>T	p.Arg618*	de novo	-	-	-	-	-	0	Novel	
MED13L	NM_015335.4	5	missense	c.6485C>A	p.Thr2162Lys	de novo	D	D	D	-	-	0	Novel	
		34	CNV	4.2-Mb deletion	-	de novo	-	-	-	-	-	-	Novel	
ZMYND11	NM_006624.5	53	frameshift	c.1438delG	p.Asp480Thrfs*3	maternal (mosaic)	-	-	D	-	-	0	Novel	
PHIP	NM_017934.7	56	missense	c.1156G>A	p.Asp386Asn	de novo	D	D	D	-	-	0	Novel	
-		51	CNV	9p 14.1-Mb del 571-kb dup	-	de novo	-	-	-	-	-	-	Novel	
EHMT1	NM_24757.4	52	CNV	9q 773.8-kb del	-	de novo	-	-	-	-	-	-	Novel	
NAA50	NM_025146.4	19	nonsense	c.93C>G	p.Tyr31*	de novo	-	-	-	-	-	-	Novel	

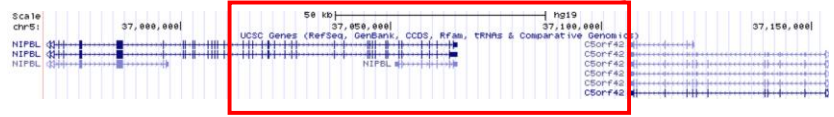
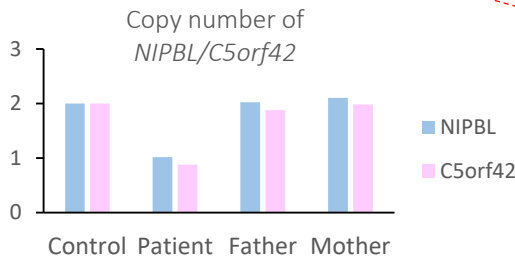
Table 1. Pathogenic variants were identified in this study.

SIFT, Sorting Intolerant From Tolerant (<http://sift.bii.a-star.edu.sg/>); PolyPhen-2, PolymorphismPhenotyping v2 (<http://genetics.bwh.harvard.edu/pph2/>); MutationTaster (<http://www.mutationtaster.org/>); ESP6500, National Heart, Lung, and Blood Institute (NHLBI) Exome Sequencing Project (ESP) Exome Variant Server (<http://evs.gs.washington.edu/EVS/>); ExAc browser (<http://exac.broadinstitute.org/>); 575 in-house, in-house 575 Japanese control exome dataset

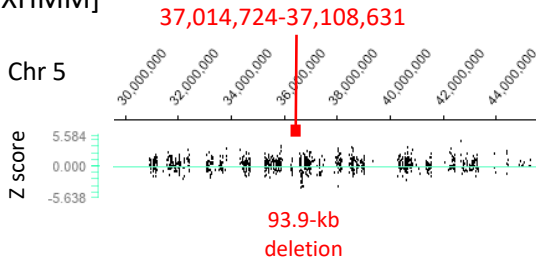


Supplementary Figure S1. Abnormal *NIPBL* transcripts generated by splice site variants. Abnormal transcripts were confirmed in (a) Patient 15 with c.3121+1G>A in *NIPBL* and (b) Patient 28 with c.7410+4A>G in *NIPBL*. The upper schematic shows a partial gene structure with the splicing variant. The middle schematic shows the mutant and wild-type cDNA. The lower image shows wild-type and mutant cDNA products in electrophoresed gels. The asterisk (*) indicates aberrant transcripts of 374 bp, generated by exon 10 skipping (a), and 971 bp, generated by exon 43 skipping (b). *ACT1* was used as the control.

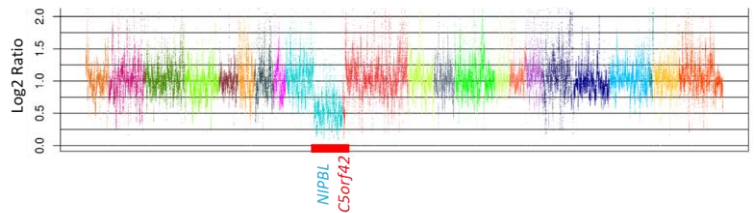
a Patient 9



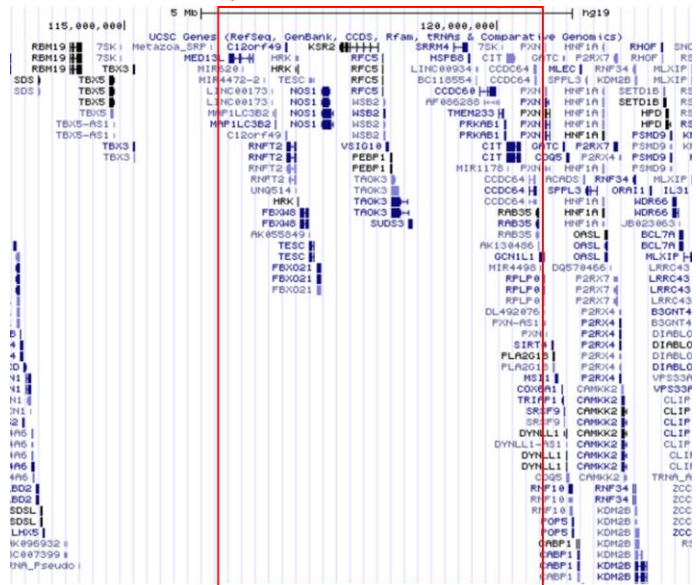
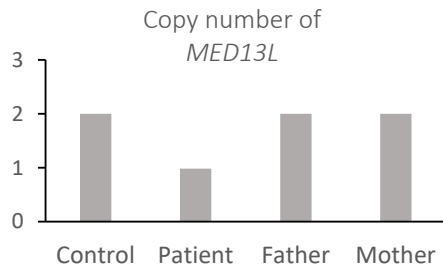
[XHMM]



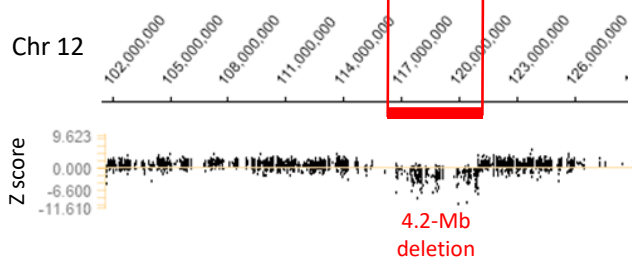
[Nord]



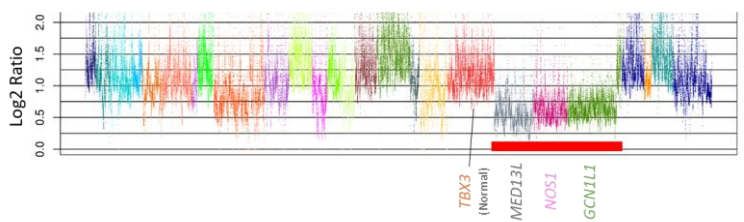
b Patient 34



[XHMM]



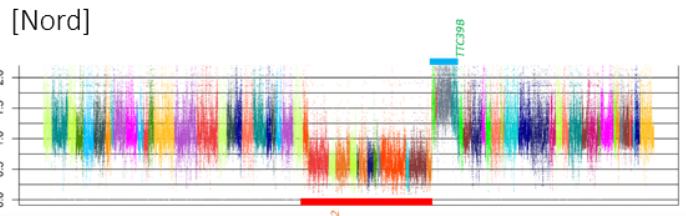
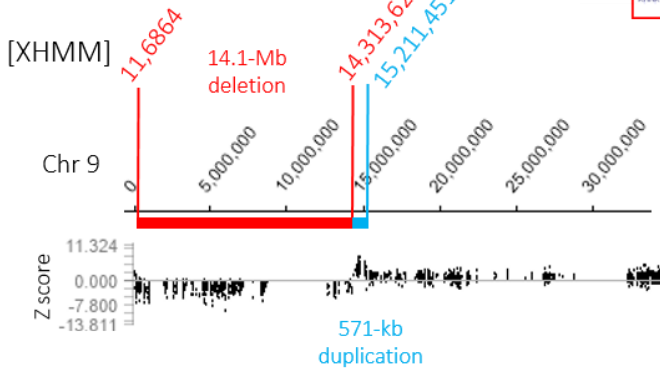
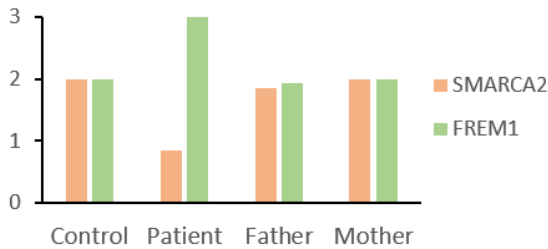
[Nord]



c Patient 51



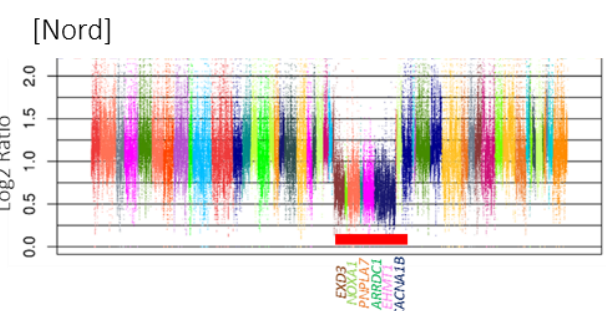
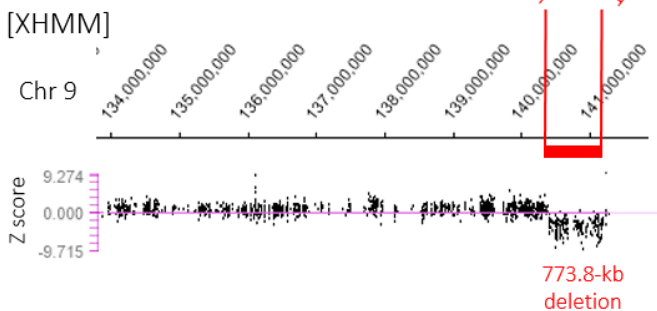
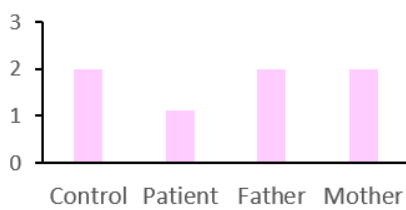
Copy number of *SMARCA2/FREM1*



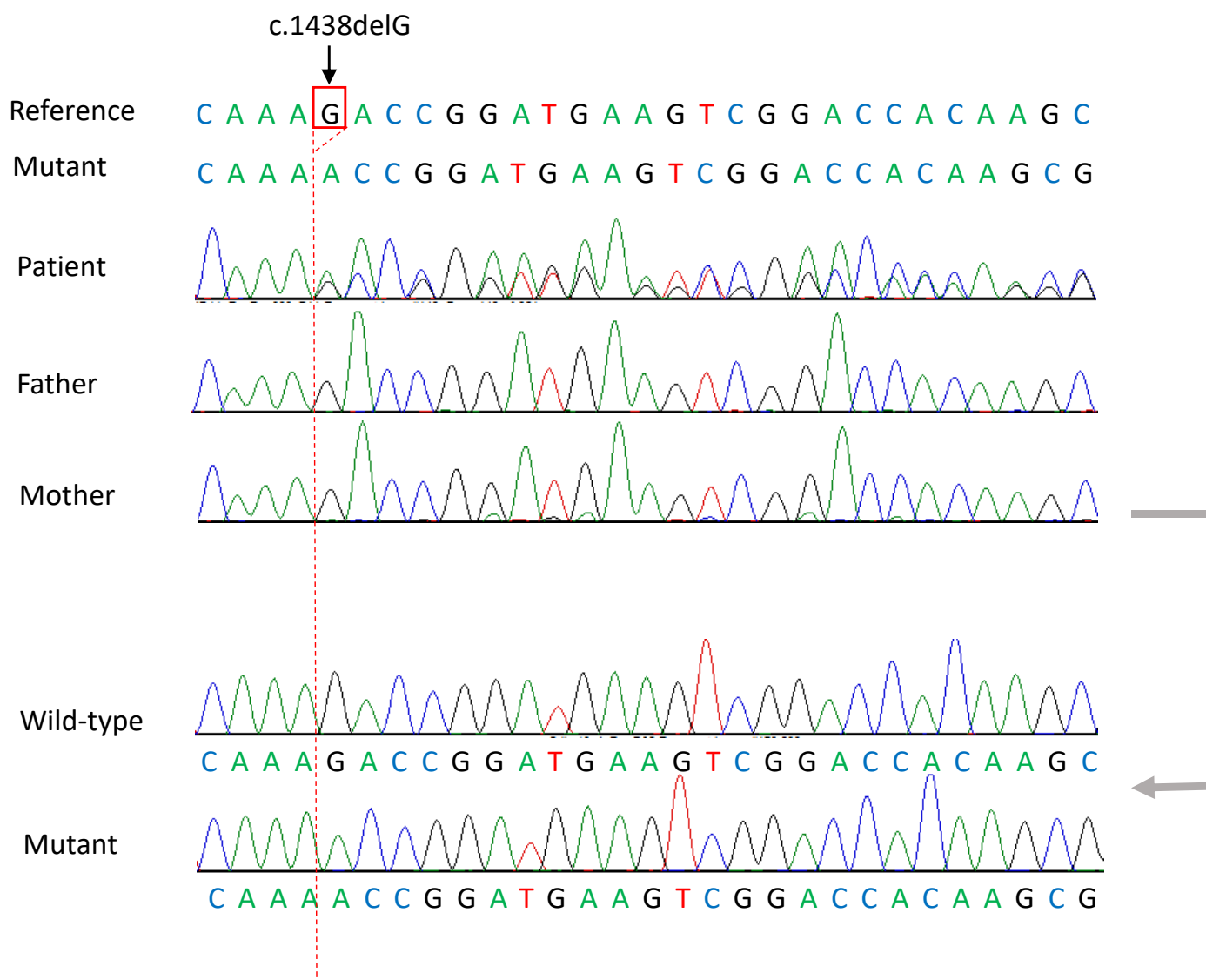
d Patient 52



Copy number of *EHMT1*



Supplementary Figure S2. Four patients with pathogenic CNVs detected using WES data. Red squares/bars indicates deletions, and blue squares/bars indicates duplications identified usingXHMM and Nord programs. Copy number variations (CNVs) were confirmed by qPCR. (a) Patient 9 had a *de novo* 93.9-kb deletion at 5p13.2 corresponding to exons 22 to 47 of *NIPBL* and the last exon of *C5orf42*. *NIPBL* and *C5orf42* deletion were confirmed by qPCR. (b) Patient 34 possessed a *de novo* 4.2-Mb deletion involving 40 RefSeq genes including *MEDI3L* at 12q24.1-q24.23. *MEDI3L* deletion was confirmed by qPCR. (c) Patient 51 had a *de novo* 14.1-Mb deletion at 9p24.3-p22.3 involving 44 RefSeq genes adjacent to a 571-kb duplication at 9p22.3 encompassing four genes. *SMARCA2* deletion and *FREMI1* duplication were confirmed by qPCR. (d) Patient 52 showed a *de novo* 773.8-kb deletion at 9q34.3 involving 14 RefSeq genes including *EHMT1*. *EHMT1* deletion was confirmed by qPCR.



Supplementary Figure S3. A frameshift *ZMYND11* variant in Patient 53 and his mosaic mother with low level mosaicism. Heterozygous c.1438delG was detected in electropherograms of Patient 53. Double sequences were detected in the maternal electropherogram. By cloning the PCR product in the mother, wild-type and mutant alleles were clearly recognized by Sanger sequencing.

Supplementary Table S1. Pathogenic variants and clinical features in all 57 patients. Please see the separate file. Pathogenic variants and clinical features of CdLS are summarized.

Patient	Sequenced base(bp)	Mean depth	Covered regions (%)		
			> 5 reads	> 10 reads	> 20 reads
1	2,717,491,258	81.19	98.1	97.6	95.9
2	2,345,160,622	70.06	98.1	97.5	94.9
3	2,410,547,560	72.02	98.1	97.5	95
4	2,193,943,963	65.55	98.1	97.3	94.3
5	2,134,650,052	63.77	98	97.2	93.4
6	2,278,525,905	68.07	98	97.3	94.7
7	3,327,143,568	99.4	98.3	98	96.9
8	2,353,682,334	70.32	98.1	97.5	95
9	1,956,621,164	58.46	97.9	97	92.7
10	2,467,364,092	73.71	97.9	97.2	94.1
11	2,163,878,827	64.65	97.9	96.9	92.7
12	2,386,979,976	71.31	97.9	97.2	94.2
13	2,709,790,390	80.96	98.1	97.5	95.2
14	2,271,433,984	67.86	97.9	97.1	93.6
15	2,497,750,149	74.62	98	97.3	94.5
16	2,401,689,900	71.75	98	97.3	94
17	3,068,833,794	91.68	98.2	97.7	96
18	2,811,745,691	84	98	97.5	95.4
19	2,244,406,012	67.05	98	97.2	93.3
20	2,515,145,707	75.14	98	97.3	94.8
21	2,304,367,691	68.84	98	97.4	94.5
22	2,071,779,476	61.9	98	97.2	93.3
23	2,077,593,792	62.07	98	97.1	93
24	2,584,558,871	77.22	98	97.5	95.3
25	2,214,779,528	66.17	97.9	96.9	92.2
26	3,250,938,863	97.12	98.1	97.7	96
27	2,588,522,835	77.33	98.1	97.4	94.8
28	2,617,702,774	78.21	97.9	97.1	94.4
29	3,294,551,016	98.43	98	97.5	95.8
30	2,217,645,104	66.25	97.8	96.1	88.2
31	2,037,671,095	60.88	97.8	96.5	90.7
32	2,627,629,431	78.5	98	97.3	94.3
33	1,924,415,550	57.49	97.9	96.8	91.2
34	2,743,248,459	81.96	97.8	96.7	92.2
35	3,250,384,892	97.11	98.1	97.7	96.1
36	2,232,039,428	66.68	98.1	97.3	93.5
37	2,722,699,721	81.34	98	97.5	95
38	2,480,268,680	74.1	98	97.3	94.4
39	3,425,858,008	102.35	98.2	97.7	96.2
40	2,127,989,922	63.57	98	97	92.4
41	2,140,157,321	63.94	98	96.9	92.1
42	2,970,702,586	88.75	98.1	97.6	95.8
43	3,052,462,950	91.19	98.1	97.6	95.6
44	2,956,719,611	88.33	98.1	97.6	95.7
45	2,708,263,123	80.91	98.1	97.5	95.2
46	2,760,250,251	82.46	98	97.5	95.5
47	2,438,746,246	72.86	98	97.3	94.3
48	2,902,940,061	86.73	98.1	97.6	95.6
49	3,442,610,124	102.85	98	97.5	95.5
50	3,625,730,620	108.32	98.1	97.6	95.8
51	2,395,445,229	71.57	98	97.3	94.5
52	2,221,757,172	66.38	97.9	97	93.3
53	2,226,712,912	66.52	98	97.1	93.4
54	2,934,068,828	87.66	98.3	97.9	95.4
55	2,759,645,091	82.45	98.3	97.8	94.9
56	3,109,737,458	92.91	98.1	97.6	95.6
57	2,900,351,453	86.65	98.1	97.4	94.5

Supplementary Table S2. WES performance. Whole exome sequencing (WES) was performed in all 57 patients with suspected CdLS. Mean read depth of protein coding regions ranged from 57.49× to 108.32×, with an average 94.3% of target bases sequenced by 20 or more reads.

		total	G (WT)	Deletion (Mut)	Other substitutions			
					A	C	T	N
Patient	read count (%)	27211	14629 (53.8)	12514 (46.0)	30 (0.1)	24 (0.1)	13 (0.0)	1 (0.0)
Mother	read count (%)	27596	24718 (89.6)	2835 (10.3)	20 (0.1)	14 (0.1)	9 (0.0)	0 (0.0)
Father	read count (%)	29548	29500 (99.8)	0	30 (0.1)	6 (0.0)	10 (0.0)	2 (0.0)
Control	read count (%)	45574	45507 (99.9)	1 (0.0)	32 (0.1)	13 (0.0)	19 (0.0)	2 (0.0)

Supplementary Table S3. Mutant read frequencies of *ZMYND11*. Deep sequencing indicated a mutant allele read frequency of 10.3% in the mother and 46.0% in Patient 53.

<i>Sex</i>	female	female	
<i>age</i>	24y	6y	
<i>Clinical score</i>	8	9	
<i>Classification</i>	molecular test	non-classic	
<i>MED13L alteration</i>	c.6485C>A, p.(Thr2162Lys)	4.2-Mb deletion	
<i>Inheritance</i>	<i>de novo</i>	<i>de novo</i>	
Dysmorphic features			
<i>MED13L</i> features	broad/prominent forehead	+	-
	bitemporal narrowing	+	+
	horizontal eyebrows	-	-
	upslanting palpebral fissures	-	+
	long down palpebral fissures	-	-
	enlargement of the palpebral fissures	-	-
	everted lower eyelids	-	-
	full cheeks	+	-
	bulbous nasal tip	-	+
	deep philtrum	-	-
	wide open mouth	-	-
	protruding tongue	-	-
	cupid-bow upper lip	-	-
	CdLS features	microcephaly	+
synophrys		+	+
hyghly arched eyebrows		-	+
long curly eyelashes		+	+
anteverted nostrilis		+	+
	long philtrum	-	-
	downturned corners of the mouth	-	-
	short neck	-	+
Upper limb abnormalities	+	+	
	5th finger clinodactyly	5th finger clinodactyly	
Congenital heart defects	-	+	
	bradycardia	ASD	
Hypotonia	+	+	
Age for independent walking	not able to walk	60 months	
Speech delay	+	+	
	only vocals ; "ma" "pa"	only a few sounds	
Epilepsy	+	-	
	from4-6y		
Developmental delay	+	+	
Intellectual disability	+	+	
Brain MRI findings	NA	NA	
Others	recurrent otitis	-	
Death or alive	death	alive	

Abbreviations: ASD, atrial septal defects; NA, Non available

Supplementary Table S4. Comparison of clinical features of *MED13L* haploinsufficiency syndrome and CdLS in two patients with *MED13L* abnormality. Pathogenic variants were identified in *MED13L* in two patients: c.6485C>A, p.Thr2162Lys in Patient 5, and a 4.2-Mb deletion involving *MED13L* in Patient 34. Both patients shared several clinical features of *MED13L* haploinsufficiency syndrome as well as CdLS.

	<i>Gene</i>	<i>Gene-phenotype relationships [OMIM]</i>	<i>Function of proteins</i>
Cohesin complex and its regulation factors	<i>NIPBL</i>	Cornelia de Lange syndrome 1	cohesin loading to the genome
	<i>SMC1A</i>	Cornelia de Lange syndrome 2	cohesin ring components
	<i>SMC3</i>	Cornelia de Lange syndrome 3	cohesin ring components
	<i>HDAC8</i>	Cornelia de Lange syndrome 5	SMC3 is deacetylated to be reused the cohesin by following cycle
	<i>RAD21</i>	Cornelia de Lange syndrome 4	cohesin ring components
	<i>STAG2</i>	Neurodevelopmental disorder, X-linked, with craniofacial abnormalities	cohesin ring components
	<i>ESPL1</i>	-	cleave RAD21 of the centromeric cohesin and open the cohesin ring
Chromatin modification factors	<i>ANKRD11</i>	KBG syndrome	transcription inhibition by interacting with histone deacetylases (HDACs) and histone molecules
	<i>ARID1B</i>	Coffin-Siris syndrome 1	components of BAF complex, bind close to transcriptional start sites and responsible for chromatin remodeling
	<i>EP300</i>	Rubinstein-Taybi syndrome 2	encoding acetyltransferase to mark H3K18 and H3K27 acetylation
	<i>KMT2A</i>	Wiedemann-Steiner syndrome	encoding methyltransferase to mark H3K4 methylation
	<i>ZMYND11</i>	Mental retardation, autosomal dominant 30	the SWI/SNF chromatin-remodeling complex to reset the chromatin to a repressive state to prevent further transcription
	<i>PHIP</i>	Developmental delay, intellectual disability, obesity, and dysmorphic features	H3K4 methylation-binding protein
Transcriptional regulation factors	<i>AFF4</i>	CHOPS syndrome	components of the super elongation complex (SEC), RNAP2 pausing release
	<i>BRD4</i>	-	binding super-enhancers with NIPBL and co-regulate developmental gene expression
	<i>MED13L</i>	Mental retardation and distinctive facial features with or without cardiac defects	crucial link between transcription factors,coactivators, and the main mediator complex
	<i>SETD5</i>	Mental retardation, autosomal dominant 23	interacts with the PAF1 co-transcriptional complex
	<i>TAF6</i>	Alazami-Yuan syndrome	components of TFIID, binding promoter with RANP2 and transcriptional initiation

Supplementary Table S5. Function of genes associated with CdLS and CdLS-like. A total of 18 genes were classified to three functional categories: cohesin complex and its regulation, chromatin modification, and transcriptional regulation. Three genes (*ZMYND11*, *MED13L*, and *PHIP*) associated with diseases other than CdLS and CdLS-like were categorized to chromatin modification factors or transcriptional regulation factors. *ZMYND11* was categorized to chromatin modification factors, of which the SWI/SNF chromatin-remodeling complex resets chromatin to a repressive state to prevent further transcription. *MED13L* was categorized to transcriptional regulation factors showing a crucial link to EP300 (as a histone modification factor). *PHIP* was categorized to chromatin modification factors (as an H3K4 methylation-binding protein).

Supplementary Table S1. Pathogenic variants and clinical features in all 57 patients.

Patient	1	2	3	4	5	6	7	8	9	10	11	12	13	14
Sex	female	male	male	male	female	female	male	male	female	female	female	female	male	female
Age (at point of study entry)	59y	8y	1y 1m	3y 10m	24y	7827	21y	17y	4y	8y	2y 6m	5y 9m	12y	3y
Clinical score	10	13	14	12	8	9	11	11	12	12	4	13	9	9
Classification	non-classic	classic	classic	classic	molecular testing	non-classic	classic	classic	classic	classic	molecular testing	classic	non-classic	non-classic
Gene	SETD5	NIPBL	NIPBL	NIPBL	MED13L	EP300	NIPBL	NIPBL	NIPBL	NIPBL	SMC1A	undetermined	NIPBL	undetermined
Variant type	nonsense	missense	nonsense	missense	missense	frameshift	missense	missense	missense	missense	frameshift	missense	-	frameshift
Mutation (hg19)	c.1852C>T	c.6893G>A	c.6179dup	c.7699T>G	c.6485C>A	c.7014_7028del	c.5595G>T	c.6620T>C	93.9-kb deletion	c.5174delA	c.1152C>G	-	c.2479_2480del	-
Protein	p.Arg618*	p.Arg2298His	p.His2060Glnfs*4	p.Tyr2567Asp	p.Thr2162Lys	p.His2338_Pro2342del	p.Arg1865Ser	p.Met2207Thr	-	p.Lys1725Serfs*17	p.Lys362Asn	-	p.Arg827Glyfs*2	-
Dysmorphic features														
synophrys	+	+	+	-	+	+	+	+	+	+	-	+	+	+
highly arched eyebrows	+	+	+	+	-	+	+	+	+	-	+	-	+	+
long curly eyelashes	+	+	+	+	+	+	+	+	+	+	-	+	+	+
ptosis	-	-	-	-	-	-	-	-	+	-	+	-	-	-
cleft lip	-	-	-	-	-	-	-	-	-	-	-	-	-	-
cleft palate	-	-	-	-	-	-	-	-	-	-	-	-	+	-
microcephaly	-	+	+	+	+	+	-	+	+	+	-	+	+	+
anteverted nostrils	+	+	+	+	+	+	-	+	+	+	-	+	+	+
depressed nasal bridge	+	-	+	-	-	-	+	-	+	-	-	-	+	+
long philtrum	+	+	+	+	-	-	+	+	-	+	-	+	-	+
thin upper lip	+	+	+	+	-	+	-	-	+	+	-	+	+	-
downturned corners of the mouth	+	+	+	+	-	+	-	-	-	+	-	+	+	-
micrognathia	-	-	-	+	+	-	-	-	-	+	-	+	-	+
short neck	+	+	-	-	-	+	+	+	+	+	-	+	-	+
high palate	-	-	-	-	-	+	+	-	+	-	+	+	-	-
widely spaced or absent teeth	-	-	-	-	NA	-	-	-	-	-	-	-	-	+
others					low set ears									
Growth														
weight below 5th percentile for age	+	-	+	+	-	-	-	-	+	+	+	+	-	-
height or length below 5th percentile for age	-	+	+	+	+	+	+	+	+	+	-	+	-	-
prenatal growth retardation	-	+	+	+	-	NA	+	-	+	+	+	+	+	-
others														
Development														
intellectual disability	+	-	NA	+	+	+	+	-	+	+	-	+	+	+
developmental delay or mental retardation	+	-	+	+	+	+	+	+	+	+	+	+	+	+
Behavior														
attention deficit disorder	+	+	NA	+	+	+	-	+	NA	+	+	+	+	+
anxiety	+	+	NA	+	+	+	+	+	NA	+	+	+	-	+
aggression	-	-	NA	+	+	+	+	+	NA	-	-	-	-	+
self-injurious behavior	-	+	NA	-	-	+	+	-	NA	+	+	+	+	+
autistic behavior	+	-	NA	-	-	+	+	-	NA	+	-	-	-	+
Limb abnormalities														
absence of forearms	-	-	-	-	NA	-	-	-	+	-	-	-	-	-
small hands and/or feet	-	-	-	-	NA	-	-	-	-	+	-	-	+	-
oligodactyly	-	-	-	-	NA	-	-	-	-	+	-	-	+	-
5th finger clinodactyly	-	+	+	-	+	+	+	+	-	-	-	-	-	-
abnormal palmar crease	-	+	+	-	NA	+	+	+	-	+	-	-	+	-
syndactyly	-	-	+	+	NA	+	-	+	-	+	-	+	-	-
phocomelia	-	-	-	-	NA	-	-	-	-	-	-	-	-	-
limited elbow extension	-	-	-	-	NA	-	+	-	-	-	-	-	-	-
proximally placed thumbs	-	-	+	-	NA	+	+	-	-	-	-	-	-	-
others					club feet				unilateral absence of hand					

Neurosensory–Skin															
ptosis	-	-	-	-	-	-	-	-	-	-	-	+	-	+	-
myopia	-	-	NA	-	+	+	-	-	-	+	+	+	-	-	+
deafness or hearing loss	-	-	NA	-	-	+	-	-	-	+	+	-	-	+	-
seizures	-	-	-	+	+	-	-	+	+	+	+	-	-	+	+
hirsutism, generalized	-	+	+	-	+	+	+	+	+	-	+	+	+	+	+
others											-				
Genitourinary															
cryptorchidism	-	+	+	-	-	-	+	-	-	-	-	-	-	+	-
hypoplastic (small) genitalia	-	-	+	+	-	-	-	-	-	-	-	-	-	+	+
renal abnormalities	-	-	-	-	-	-	-	-	-	-	-	-	-	-	-
others															
Cardiovascular															
ventricular septal defects	+	-	-	-	-	NA	-	-	-	-	-	-	-	-	-
atrial septal defects	-	-	-	-	-	NA	-	-	-	-	-	-	-	-	-
pulmonic ste-sis	-	-	+	-	-	NA	-	+	-	-	-	-	-	-	-
tetralogy of Fallot	-	-	-	-	-	NA	-	-	-	+	-	-	-	-	-
hypoplastic left heart	-	-	-	-	-	NA	-	-	-	-	-	-	-	-	-
bicuspid aortic valve	-	-	-	-	-	NA	-	-	-	-	-	-	-	-	-
others															
Others															
language delay	+	-	+	-	+	+	+	-	+	-	+	+	+	+	+
diaphragmatic hernia	-	-	-	-	-	-	-	-	-	-	-	-	-	-	-
gastroesophageal reflux	-	+	-	+	+	-	+	+	+	+	+	+	+	+	+
others															

Abbreviations: y, years; m, months; NA, not available

Patient	29	30	31	32	33	34	35	36	37	38	39	40	41	42
Sex	female	male	male	male	male	female	female	male	female	female	male	male	male	female
Age (at point of study entry)	25y	43y	1y 1m	16y	13y	6y	9y	26y	3y	14y	3y 9m	5y 10m	NA	15y
Clinical score	9	12	13	7	10	9	9	13	11	13	11	12	10	13
Classification	non-classic	classic	classic	molecular testing	non-classic	non-classic	non-classic	classic	classic	classic	classic	classic	non-classic	classic
Gene	undetermined	undetermined	NIPBL	undetermined	undetermined	MED13L	undetermined	NIPBL	undetermined	NIPBL	NIPBL	undetermined	NIPBL	SMC1A
Variant type	-	-	frameshift	-	-	CNV	-	nonsense	-	nonsense	nonsense	-	missense	missense
Mutation (hg19)	-	-	c.6653_6655del	-	-	4.2-Mb deletion	-	c.5509C>T	-	c.826C>T	c.190C>T	-	c.6343G>T	c.1487G>A
Protein	-	-	p.Asn2218del	-	-	-	-	p.Arg1837*	-	p.Gln276*	p.Gln64*	-	p.Gln2115Cys	p.Arg496His
Dysmorphic features														
synophrys	+	+	+	+	+	+	+	+	+	+	+	+	+	+
highly arched eyebrows	+	+	+	+	+	+	+	+	+	+	+	+	+	-
long curly eyelashes	-	+	+	-	-	+	-	+	+	+	+	+	+	+
ptosis	-	-	-	-	-	-	-	-	-	-	-	-	-	-
cleft lip	-	-	-	-	-	-	-	-	-	-	-	-	-	-
cleft palate	-	-	-	-	-	-	+	-	-	-	-	+	-	-
microcephaly	+	-	+	-	+	-	-	+	+	+	+	+	-	+
anteverted nostrils	-	-	+	-	-	+	-	+	-	+	+	+	+	-
depressed nasal bridge	-	+	+	-	-	-	+	+	-	+	-	-	-	+
long philtrum	-	+	+	-	+	-	-	+	+	+	+	+	-	+
thin upper lip	+	+	+	+	+	-	-	+	+	+	-	+	+	+
downturned corners of the mouth	+	+	+	+	+	-	-	+	+	+	-	+	-	+
micrognathia	-	-	+	-	+	-	-	+	-	+	-	-	-	-
short neck	+	+	-	+	-	+	-	+	+	+	+	-	-	-
high palate	-	+	-	+	-	-	+	-	-	-	+	-	+	-
widely spaced or absent teeth	-	-	-	-	-	-	+	-	-	+	-	-	-	-
others						low set ears								
Growth														
weight below 5th percentile for age	+	-	+	+	+	-	+	+	+	+	+	+	+	+
height or length below 5th percentile for age	+	-	-	+	+	+	+	+	+	+	+	+	+	+
prenatal growth retardation	+	+	+	-	-	+	+	+	+	+	+	-	+	-
others														
Development														
intellectual disability	+	+	NA	+	+		+	+	+	+	+	+	+	+
developmental delay or mental retardation	+	+	+	+	+	+	+	+	+	+	+	+	+	+
Behavior														
attention deficit disorder	+	+	NA	+	+	+	-	+	+	+	+	+	-	+
anxiety	+	+	NA	-	-	+	-	+	+	+	-	+	-	+
aggression	-	-	NA	-	-	+	+	+	+	-	+	-	-	-
self-injurious behavior	+	-	NA	-	+	-	+	+	-	+	+	-	-	+
autistic behavior	-	+	NA	+	+	-	-	+	-	-	+	-	-	-
Limb abnormalities														
absence of forearms	-	-	-	-	-	-	-	-	-	-	-	-	-	-
small hands and/or feet	-	-	-	-	-	-	-	+	-	-	-	-	-	-
oligodactyly	+	-	-	-	-	-	+	-	-	-	-	-	-	-
5th finger clinodactyly	-	+	+	-	+	+	-	-	-	-	-	-	-	+
abnormal palmar crease	-	-	+	+	-	+	+	+	-	+	-	-	-	-
syndactyly	-	+	-	-	-	-	+	+	-	+	-	-	+	-
phocomelia	-	-	-	-	-	-	-	-	-	-	-	-	-	-
limited elbow extension	+	+	-	-	+	-	-	+	-	+	-	-	-	+
proximally placed thumbs	-	-	+	-	+	-	+	+	-	+	-	-	-	-
others		asymmetry									campodactyly			

Neurosensory–Skin															
ptosis	-	-	-	-	-	-	-	-	-	-	-	-	-	-	-
myopia	-	-	-	+	-	-	-	-	-	-	-	-	-	-	-
deafness or hearing loss	-	-	-	+	-	-	-	-	+	-	+	-	-	+	
seizures	+	-	+	+	-	-	-	-	+	-	-	+	-	-	
hirsutism, generalized	+	+	-	+	-	+	-	+	+	+	+	+	-	+	
others								coloboma		white lesions		lacrimal glands			
Genitourinary															
cryptorchidism	-	-	+	+	-	-	-	+	-	-	-	-	+	-	-
hypoplastic (small) genitalia	-	+	+	-	-	-	-	+	+	-	-	-	-	-	+
renal abnormalities	-	+	-	+							+	-	-	-	
others								hydrocele							
Cardiovascular															
ventricular septal defects	-	-	-	-	-	-	-	+	-	-	-	-	-	-	-
atrial septal defects	-	-	-	-	-	+	-	+	+	-	-	+	-	-	
pulmonic ste-sis	-	-	-	-	-	-	-	+	-	-	+	-	-	-	
tetralogy of Fallot	-	-	-	-	-	-	-	-	-	-	-	-	-	-	
hypoplastic left heart	-	-	-	-	-	-	-	-	-	-	-	-	-	-	
bicuspid aortic valve	-	-	-	-	-	-	-	-	-	-	-	-	-	-	
others															
Others															
language delay	+	-	+	+	+	-	+	+	+	+	+	+	-	+	+
diaphragmatic hernia	-	-	-	+	-	-	-	-	-	-	-	-	-	-	-
gastroesophageal reflux	+	+	-	-	+	+	+	+	+	+	+	-	+	+	+
others								scoliosis				small cerebellum			scoliosis

Patient	43	44	45	46	47	48	49	50	51	52	53	54	55	56	57
Sex	male	male	male	female	female	male	female	female	female	female	male	male	female	male	male
Age (at point of study entry)	11y	4y	8m	6m	16y	18y	8y	11y	7y	5y	5y 10m	7y	4y 6m	11y	6y
Clinical score	9	14	10	14	5	9	10	6	7	5	15	6	10	6	9
Classification	non-classic	classic	non-classic	classic	molecular testing	non-classic	non-classic	molecular testing	molecular testing	molecular testing	classic	molecular testing	non-classic	molecular testing	non-classic
Gene	ANKRD11	undetermined	NIPBL	undetermined	undetermined	NIPBL	NIPBL	NIPBL	-	EHMT1	ZMYND11	NIPBL	NIPBL	PHIP	undetermined
Variant type	nonsense	-	missense	-	-	frameshift	missense	missense	CNV	CNV	frameshift	splicing	missense	missense	-
Mutation (hg19)	c.5434C>T	-	c.6027G>C	-	-	c.8325_8326delinsT	c.6448C>G	c.6893G>A	9p 14.1-Mb deletion, 571-kb duplication	9q 773.8-Kb deletion	c.1438delG	c.5329-15A>G	c.7079G>T	c.1156G>A	-
Protein	p.Gln1812*	-	p.Leu2009Phe	-	-	p.Lys2775Asnfs*4	p.Leu2150Val	p.Arg2298His	-	-	p.Asp480Thrfs*3	-	p.Glu2360Val	p.Asp386Asn	-
Dysmorphic features															
synophrys	+	+	+	+	-	+	+	+	+	+	+	+	+	+	+
highly arched eyebrows	-	+	+	+	+	+	+	+	-	-	+	+	+	-	+
long curly eyelashes	+	+	+	+	+	+	+	-	-	+	+	+	+	+	+
ptosis	-	-	-	-	-	-	-	-	-	-	-	-	-	-	-
cleft lip	-	-	-	-	-	-	-	-	-	-	-	-	-	-	-
cleft palate	-	-	-	-	-	-	-	-	-	-	-	-	-	-	-
microcephaly	+	+	+	+	+	-	-	-	-	-	+	-	+	-	+
anteverted nostrils	-	+	+	+	-	-	+	+	+	-	+	+	-	+	+
depressed nasal bridge	+	+	+	+	-	+	-	-	-	+	-	+	-	+	-
long philtrum	+	+	-	+	-	+	-	-	+	-	+	-	+	-	-
thin upper lip	+	+	-	+	-	-	+	-	-	-	+	-	+	-	+
downturned corners of the mouth	+	+	+	+	-	-	+	-	-	-	+	-	+	-	-
micrognathia	-	+	-	-	-	-	+	-	-	-	+	-	+	-	-
short neck	-	-	+	-	-	+	-	-	-	-	-	-	-	+	-
high palate	+	-	-	-	-	-	-	-	-	-	-	-	-	-	-
widely spaced or absent teeth	+	-	-	-	-	+	+	-	-	-	-	-	-	-	-
others															macrocephaly
Growth															
weight below 5th percentile for age	-	+	+	+	+	-	-	-	-	-	+	+	+	-	-
height or length below 5th percentile for age	-	+	+	+	+	+	-	-	-	-	-	+	+	-	-
prenatal growth retardation	+	+	+	+	+	-	+	-	-	-	+	-	+	+	-
others															obesity
Development															
intellectual disability	-	+	NA	NA	+	-	+	+	+	-	+	-	+	+	+
developmental delay or mental retardation	+	+	+	+	+	+	+	+	+	+	+	+	-	+	+
Behavior															
attention deficit disorder	+	+	NA	NA	+	+	+	+	+	+	+	-	+	+	+
anxiety	+	+	NA	NA	+	+	+	+	+	+	+	-	+	+	+
aggression	-	+	NA	NA	-	-	+	+	+	+	-	-	+	-	+
self-injurious behavior	-	-	NA	NA	-	-	+	-	+	+	+	-	+	+	-
autistic behavior	-	-	NA	NA	+	-	-	+	+	+	-	-	-	-	-
Limb abnormalities															
absence of forearms	-	-	-	-	-	-	-	-	-	-	+	-	-	-	-
small hands and/or feet	-	-	-	-	-	+	-	-	-	-	-	-	-	-	-
oligodactyly	-	-	-	-	-	-	-	-	-	-	+	-	-	-	-
5th finger clinodactyly	-	+	-	+	-	-	+	-	-	-	-	-	-	-	-
abnormal palmar crease	-	-	+	-	-	-	+	-	-	-	+	-	-	-	-
syndactyly	-	-	+	+	-	+	+	-	-	-	-	-	-	-	-
phocomelia	-	-	-	-	-	-	-	-	-	-	-	-	-	-	-
limited elbow extension	-	-	-	-	-	-	+	-	-	-	-	-	-	-	-
proximally placed thumbs	-	-	+	+	-	-	-	-	-	-	-	-	-	-	-
others	camptodactyly						sternum	asymmetry							

Neurosensory–Skin															
ptosis	-	-	-	-	-	-	-	-	-	-	-	-	-	-	-
myopia	-	-	-	-	-	+	-	-	-	-	+	-	-	-	-
deafness or hearing loss	-	+	-	-	-	-	-	-	+	+	-	-	-	-	+
seizures	+	-	-	-	+	+	-	-	-	-	-	-	-	-	+
hirsutism, generalized	-	+	-	+	+	+	+	+	-	-	+	+	+	-	+
others															
Genitourinary															
cryptorchidism	+	-	+	-	-	+	-	-	-	-	+	-	-	-	-
hypoplastic (small) genitalia	-	-	-	-	+	+	NA	-	-	-	+	-	-	-	+
renal abnormalities	-	-	-	-	-	-	-	-	-	-	-	-	-	-	-
others															
Cardiovascular															
ventricular septal defects	-	-	-	-	-	-	-	-	+	-	-	-	-	-	-
atrial septal defects	-	-	-	-	-	-	-	-	-	-	-	-	-	-	-
pulmonic ste-sis	-	-	+	-	-	-	-	-	-	-	-	-	-	-	-
tetralogy of Fallot	-	-	-	-	-	-	-	-	-	-	-	-	-	-	-
hypoplastic left heart	-	-	-	-	-	-	-	-	-	-	-	-	-	-	-
bicuspid aortic valve	-	-	-	-	-	-	-	-	-	-	+	-	-	-	-
others													aortic reflux		
Others															
language delay	-	+	NA	+	+	+	+	+	+	+	+	-	+	+	+
diaphragmatic hernia	-	-	-	-	-	-	-	-	-	-	-	-	-	-	-
gastroesophageal reflux	-	+	+	+	+	-	+	+	-	+	+	-	-	-	+
others										inguinal hernia					